Title: Dynamic *Ins2* gene activity defines β cell maturity states

Authors: Honey Modi[1]*, Chieh Min Jamie Chu[1]*, Søs Skovsø[1], Cara Ellis[1], Nicole A.J. Krentz[2], Yiwei Bernie Zhao[3], Haoning Cen[1], Noursadeghi N[1], Evgeniy Panzhinskiy[1], Xiaoke Hu[1], Derek A. Dionne[1], Yi Han Xia[1], Shouhong Xuan[4], Mark O. Huising[5,6], Timothy J. Kieffer[1], Francis C. Lynn[2], James D. Johnson[1#]
***** Equal contribution

Affiliations: [1]Diabetes Research Group, Life Sciences Institute, Department of Cellular and Physiological Sciences & Department of Surgery, University of British Columbia, Vancouver, Canada. [2]BC Children's Hospital Research Institute, Department of Surgery, University of British Columbia, Vancouver, Canada. [3]Biomedical Research Centre, Department of Cellular and Physiological Sciences & Department of Surgery, University of British Columbia, Vancouver, Canada. [4]Department of Medicine Hematology and Oncology, Columbia University Medical Center, New York, USA. [5]Department of Neurobiology, Physiology and Behavior, UC Davis, Davis, USA. [6]Department of Physiology and Membrane Biology, UC Davis, Davis, USA.

[#]**Address correspondence to:** James D. Johnson, PhD., Faculty of Medicine, Department Cellular and Physiological Sciences, The University of British Columbia, Life Sciences Institute, 5358 – 2350 Health Sciences Mall, Vancouver, British Columbia, Canada V6T 1Z3
Phone: 604 822 7187, Email: James.d.johnson@ubc.ca, Twitter: @JimJohnsonSci

Abstract Word Count: 230
Word Count: 4037
Reference Count: 54
Figure Count: 5
Keywords: Insulin production; cellular heterogeneity; single cell RNA sequencing, beta cell fragility
Blurb: Previously reported pancreatic β cell heterogeneity reflects β cell state transitions.
Declaration of Interests: The authors declare no competing interests.
Funding: Research was supported by a CIHR operating grant to J.D.J.
Acknowledgments: We thank many colleagues for helpful discussions.

Author Contributions:
HM designed studies, performed experiments, analyzed/interpreted data, and wrote the first draft of the manuscript.
CMJC designed studies, performed experiments, analyzed/interpreted data, wrote parts of the revised manuscript.
SS performed experiments, analyzed/interpreted data.
CE analyzed/interpreted data.
HC performed experiments, analyzed/interpreted data.
NAJK analyzed/interpreted data.
DAD performed experiments, analyzed/interpreted data.
BX analyzed/interpreted data.
XH performed experiments.
NN performed experiments and analyzed/interpreted data.
EP supervised work and analyzed/interpreted data.
YX analyzed/interpreted data.
SX provided a key reagent.
MOH provided a key reagent, designed studies, and analyzed/interpreted data.
TJK supervised work.
FCL supervised work and analyzed/interpreted data.
JDJ conceived the project, designed studies, interpreted data, edited the manuscript, and is the guarantor of this work.

Abstract

Heterogeneity within specific cell types is common and increasingly apparent with the advent of single cell transcriptomics. Transcriptional and functional cellular specialization has been described for insulin-secreting β cells of the endocrine pancreas, including so-called extreme β cells exhibiting >2-fold higher insulin gene activity. However, it is not yet clear whether β cell heterogeneity is stable or reflects dynamic cellular states. We investigated the temporal kinetics of endogenous insulin gene activity using live cell imaging, with complementary experiments employing FACS and single cell RNA sequencing, in β cells from *Ins2*^{GFP} knock-in mice. *In vivo* staining and FACS analysis of islets from *Ins2*^{GFP} mice confirmed that at a given moment, ~25% of β cells exhibited significantly higher activity at the conserved insulin gene *Ins2*. Live cell imaging captured *Ins2* gene activity dynamics in single β cells over time. Autocorrelation analysis indicated that cells displaying fluctuations in *Ins2* gene activity most commonly exhibited a frequency of 17 hours. Increased glucose concentrations stimulated more cells to oscillate and resulted in higher average *Ins2* gene activity per cell. Single cell RNA sequencing determined that *Ins2*(GFP)^{HIGH} β cells were enriched for markers of β cell maturity and had reduced expression of anti-oxidant genes. *Ins2*(GFP)^{HIGH} β cells were also significantly less viable at all glucose concentrations and in the context of ER stress. Collectively, our results demonstrate that the heterogeneity of insulin production, observed in mouse and human β cells, can be accounted for by dynamic states of insulin gene activity. Our observations define a previously uncharacterized form of β cell plasticity. Understanding the dynamics of insulin production has relevance for understanding the pathobiology of diabetes and for regenerative therapy research.

Introduction

Pancreatic β cells in the islets of Langerhans are the only source of circulating insulin, a conserved and essential hormone that is required for nutrient homeostasis and life (Szabat et al., 2016). Insulin production is highly demanding, as insulin mRNA can account for roughly half of all β cell mRNA and its synthesis, folding and processing require semi-specialized transcription factors, enzymes and cellular conditions(Boland et al., 2017; Wang et al., 2021). However, not all β cells appear the same. Indeed, functional β cell heterogeneity is well established (Benninger and Hodson, 2018), including cellular specialization for islet cell synchronization, insulin secretion, insulin production, and marker gene expression (Bader et al., 2016; Dorrell et al., 2016; Heimberg et al., 1993; Johnston et al., 2016; Kiekens et al., 1992; Kolic and Johnson, 2016; Ling et al., 1998; Pipeleers, 1992; van der Meulen et al., 2017; Wills et al., 2016; Xin et al., 2018). For example, recent *in situ* imaging has revealed the existence of extreme β cells, defined as having >2-fold *Ins2* mRNA than the median expression as measured by single-molecule fluorescence *in situ* hybridization (Benninger and Hodson, 2018; Farack et al., 2019). Single cell RNA sequencing has shown that human β cells also express *INS* over a similarly wide range (Xin *et al.*, 2018). However, it remains unclear whether this variation is the hallmark of distinct stable populations of β cells, or whether it is indicative of transitions between more labile β cell states.

To date, the vast majority of islet cell 'sub-populations' have been defined by single time-point snapshots, making it impossible to know to what extent observed β cell heterogeneity represents distinct islet cell 'fates' or variations in islet cell 'states'. This information is essential for interpreting existing and future data in the field. Using a dual *Ins1* and *Pdx1* promoter reporter construct and live cell imaging, we have previously demonstrated that mouse and human β cells can transition between less and more differentiated states over a time scale of ~24 hours (Szabat et al., 2010; Szabat et al., 2009; Szabat et al., 2011). However, the artificial promoter constructs in these early studies may not reflect endogenous gene activity, leaving open the question of whether endogenous insulin gene activity is similarly dynamic.

In this study, we measured endogenous insulin gene activity using an *Ins2*^{GFP} knock-in/knockout mouse line in which the coding sequencing of the evolutionarily conserved *Ins2* gene has been replaced with GFP (Wakae-Takada et al., 2013). Live cell imaging of dispersed cells from these mice revealed that GFP fluorescence changed over time in a sub-set of cells, suggesting that variation in *Ins2* levels results from dynamic transcriptional activity at the *Ins2* gene locus rather than stable heterogeneity. Single cell RNA sequencing was used to characterize the *Ins2*(GFP)^{HIGH} cellular state in an unbiased

way, revealing increased markers of β cell maturity as well as alterations in protein synthesis machinery and cellular stress response networks. Pancreatic β cells in the *Ins2*(GFP)^{HIGH} cellular state were also more fragile across a range of stress conditions. To the best of our knowledge, our observations are the first to define the temporal kinetics of endogenous insulin gene activity, which represents a previously uncharacterized form of β cell plasticity. Understanding the dynamics of insulin production has relevance for understanding the pathobiology of diabetes and for regenerative therapy research (Johnson, 2016).

Results

In vivo heterogeneity of insulin content in human β cell and insulin gene activity in Ins2^{GFP} mice

Heterogeneity of insulin production is an established phenomenon, and we started our study by staining human pancreas with antibodies to insulin and PDX1, a key transcription factor for β cell survival and function (Johnson et al., 2003; Szabat et al., 2012). As expected, based on single cell RNA sequencing data (Xin *et al.*, 2018) and previous single cell imaging of human β cells (Johnson et al., 2006), imaging over a large dynamic range enabled the identification of β cells with both high and low insulin protein levels in human pancreas (Fig. 1A). We have previously shown limited correlations between insulin content and Pdx1 immunofluorescence or nuclear localization in human β cells (Johnson *et al.*, 2006). In order to study insulin gene activity in living cells, we examined islets from mice in which the coding sequencing of the evolutionarily conserved *Ins2* gene has been replaced with GFP (Wakae-Takada *et al.*, 2013)(Fig. 1B). Mice lacking 1 or 2 functional *Ins2* alleles had normal glucose homeostasis (Fig. 1C), consistent with our previous studies of *Ins2* knockout mice (Mehran et al., 2012) and the ability of *Ins1* to compensate (Leroux et al., 2001). Immunofluorescence staining of pancreata from *Ins2*^{GFP} mice revealed a clear bimodal distribution of endogenous insulin production *in vivo* (Fig. 1D). Hand counting 1879 cells across 11 randomly selected islets showed that 38.7% of β cells had substantially higher GFP immunofluorescence above an arbitrary, but consistently applied, threshold (Fig. 1D). The percentage of cells with high GFP did not appear to vary as a function of islet size. We have observed similar heterogeneity when examining the β-galactosidase knock-in in to the *Ins2* locus (Mehran *et al.*, 2012). Similarly, FACS confirmed this bimodal distribution and that less than half of all β cells engage in high *Ins2* gene transcription at a given time (Fig. 1E). FACS analysis also validated that *gfp* mRNA, *Ins2* mRNA, and pre-mRNA were significantly increased in high GFP-expressing cells compared to cells expressing less GFP (Supplemental Fig. S1A), strongly suggesting that GFP protein levels accurately reflect *Ins2* mRNA in this system. We did not expect there to be a perfect correlation due to the different predicted transcription-to-protein time courses for GFP and insulin (Fig. 1H; see Supplemental Materials for calculations). Nevertheless, these data demonstrate that GFP production, reflecting the activity of the endogenous *Ins2* gene locus, is bimodal *in vivo* and *ex vivo*, with 25% of β cells showing significantly higher activity. Hereafter, we refer to cells with high GFP abundance as *Ins2*(GFP)^{HIGH}.

Live cell imaging of insulin gene activity in Ins2$^{GFP/WT}$ mice

We next generated a mouse model to examine endogenous *Ins2* activity dynamics relative to a stable background β cell marker. We crossed the *Ins2*^{GFP} knock-in line with transgenic mice with an allele wherein histone-fused mCherry is driven by the less complex *Ins1* promoter that is known to show relatively stable mCherry fluorescence in virtually all β cells (Benner et al., 2014), allowing us to track *Ins2* gene activity in real-time, while observing all β cells. As expected, immunofluorescence of intact pancreatic sections and FACS analysis of dispersed islets from *Ins2*$^{GFP/wt}$:*Ins1*-mCherry mice showed that mCherry labelled virtually all β cells, while GFP was robustly expressed in a clearly separated sub-set of β cells we deemed *Ins2*(GFP)^{HIGH} (Fig. 2A,B,C). qPCR of these FACS purified cells confirmed the expected elevated expression of GFP, *Ins2*, pre-*Ins2*, *Ins1*, and pre-*Ins1* mRNA in *Ins2*(GFP)^{HIGH} cells (Fig. 2D, Supplemental Fig. S1B). *Ins2* pre-mRNA would be expected to precede GFP fluorescence by at least 1.3 hours, as per estimations in Fig. 1H and calculations in Supplemental Information, which provides a possible explanation for the elevated pre-*Ins2* in the mCherry positive, but GFP low β cells. Both intact islets and dispersed islet cells isolated from *Ins2*$^{GFP/WT}$:*Ins1*-mCherry mice showed a similar

proportion of *Ins2*(GFP)^{HIGH} and *Ins2*(GFP)^{LOW} cells that we observed *in vivo*, demonstrating that this heterogeneity was not altered by isolation or dispersion/culture.

A high-throughput, live cell imaging system with environmental control was used to study dispersed islet cells from *Ins2*$^{GFP/WT}$:*Ins1*-mCherry mice. Remarkably, live cell imaging over ~3 days identified a sub-set of β cells that transitioned in and out of *Ins2*(GFP)^{HIGH} activity states over the course of 36-hour long recordings (Fig. 2E, Supplemental Fig. S2A, B). Analysis of 547 cells with various cellular behavior metrics as variables identified 3 distinct clusters of *Ins2* gene activity (Supplemental Fig. S2C, D). While testing for viability of the *Ins2*$^{GFP/WT}$ β cells, we noticed GFP fluorescence in *Ins2*$^{GFP/WT}$ cells sometimes rapidly decreases just prior to cell death. Therefore, in a larger study, we used propidium iodide, a dye which permits the real-time detection of the terminal stage of cell death, to identify changes in GFP fluorescence that are not associated with cell death (Fig. 3A). As propidium iodide emits red fluorescence at 636 nm, we used *Ins2*$^{GFP/WT}$ mice without *Ins1*-mCherry for these experiments. We chose the heterozygous *Ins2*$^{GFP/WT}$ genotype to keep the experiment as close as possible to wild-type studies. Dispersed islets from *Ins2*$^{GFP/WT}$ mice were studied for up to 4 days, imaging cells at 5-minute intervals. Similar to our pilot study, we identified β cells which transitioned between high and low expression states over the course of recordings (Fig. 3C). We tracked and quantified fluorescence intensities of Hoechst, GFP, propidium iodide in 2115 individual cells, confirming a bimodal distribution of mean GFP fluorescence in the cellular population (Fig. 3D) we found in our FACS analysis. Quantification of other GFP wavelength parameters, including autocorrelation function (ACF) and full width at half maximum (FWHM) revealed groups of cells with fluctuating *Ins2* gene activity (Fig. 3E). We combined K-means clustering with principal component analysis (PCA), to reveal 4 clusters displaying distinct cellular behaviors (Supplemental Fig. S3A, B). Collectively, our long-term live cell imaging demonstrates significant dynamic fluctuations in the activity of the endogenous *Ins2* locus in primary β cells, demonstrating that the apparently heterogeneity observed *in vivo* is not necessarily stable.

Autocorrelation analysis of fluctuations in Ins2 gene dynamics

The observation of fluctuations in *Ins2* gene activity in some β cells within our 4-day time window prompted us to determine the most common oscillation frequencies in *Ins2*$^{GFP/WT}$ β cells. We performed autocorrelation analysis on GFP fluorescent intensity over time in *Ins2*$^{GFP/WT}$ β cells which had at least one oscillation during the imaging period (Fig. 4A) and found that 357 (17%) out of 2115 cells had at least one oscillation, of which 226 had oscillation periods of 8-20 hours. The most common frequency fell within the 12-16 hour bin, with an average of ~17 hours across all oscillating cells (Fig. 4B), possibly suggesting this oscillation behavior may be diurnal in nature. Interestingly, we also found that cells which oscillated had significantly higher GFP fluorescent intensity in comparison to non-oscillating cells (Fig. 4B). Fluctuations in Hoechst fluorescence intensity, which marks DNA in cell nuclei, did not show significant correlation with GFP expression. Together, these relatively long-term live cell imaging data suggest that circadian-influenced oscillations of *Ins2* gene activity persist in culture.

Ins2 gene dynamics under various glucose and serum conditions

Glucose is a primary driver of insulin production, including insulin gene transcription (Boland *et al.*, 2017; Knoch et al., 2014). Therefore, we asked if altering glucose concentrations would impact endogenous *Ins2* gene activity in our knock-in model. We treated isolated islet cells from *Ins2*$^{GFP/WT}$ mice to multiple culture conditions, including without serum (serum-free), with serum, starvation from serum for 9 hours prior to imaging (serum-starved), and an array of glucose concentrations (0, 5, 10, 15, 20 mM). The time required for mature *Ins2* mRNA production in response to elevated glucose is still under debate, with various studies describing an increase in mature *Ins2* mRNA being detected at a range of several hours after high glucose treatments, up to ~48 hours (Evans-Molina et al., 2007; Tillmar et al., 2002). We found significantly higher *Ins2* gene activity in higher glucose concentrations under serum-containing conditions at the 48-hour mark (Fig. 5A, B). We did not find significantly higher *Ins2* gene activity in serum starved conditions, but there was still a trend towards higher gene activity in higher glucose concentrations. In serum-free and all 0 mM glucose conditions, cells died rapidly thus confounding analysis of *Ins2* gene activity (data not shown). After de-trending to control for photobleaching, a rise in *Ins2* gene activity was observed around 12 hours into the experiment in cells

cultured in higher glucose concentrations and serum, and to a lesser extent in serum starved conditions (Fig. 5A). Interestingly, we also found a slight increase in the ratio of *Ins2*(GFP)^{HIGH} cells in higher glucose concentrations, which may help explain the increase in overall *Ins2* gene activity in those conditions (Supplemental Fig. S4J). An early decrease in GFP fluorescence observed over the first 6 hours can possibly be attributed to stress the cells experience after a media change. We performed hierarchical clustering with heatmap construction and extracted individual variables and compared the treatments (Supplemental Fig. S4A-I). We found a significant decrease in higher versus lower glucose concentrations in the ACF time variable (Supplemental Fig. S4H). PCA with K-means clustering analyses did not reveal any distinct clusters (Supplemental Fig. S5A, B).

Autocorrelation analyses showed considerable difference in populations of oscillating versus non-oscillating cells in the various treatments. Of particular interest was the higher ratio of oscillating cells in higher glucose concentrations, suggesting that glucose may also influence *Ins2* gene expression volatility (Figure 5B). Combined with data in our initial *Ins2*$^{GFP/WT}$ imaging study in basal 10 mM glucose conditions, this suggests that oscillating cells may be a contributor to the increase in *Ins2* gene activity in response to high glucose (Figure 3, 4). Oscillation periods between treatments were not significantly different, but there was a trend towards higher oscillation periods in higher glucose concentrations (Supplemental Fig. S4C). We also looked at the amplitude of the oscillations by comparing the range of GFP fluorescence in oscillating cells, but we also did not find any differences (Supplemental Fig. S4B). Collectively, these results show that various glucose concentrations under serum conditions may influence *Ins2* gene activity and behavior.

Profiling β cell states with single cell RNA sequencing

To characterize the *Ins2*(GFP)^{HIGH} state in a comprehensive and unbiased way, we performed single cell RNA sequencing on FACS purified *Ins2*(GFP)^{HIGH} and *Ins2*(GFP)^{LOW} cells from islets pooled from 3 mice (Fig. 6A-E). We then examined differential gene expression as a function of *gfp* mRNA (Fig. 6D), including only single cells expressing *Ins1* mRNA which are presumably β cells or rare multi-hormonal islet cells (Fig. 6A, B). We also considered *Ins2*(GFP)^{HIGH} and *Ins2*(GFP)^{LOW} as binary categories and obtained similar results (Supplemental Fig. S8 A, B).

In 8 week-old *Ins2*$^{GFP/WT}$ mice, pathway enrichment analysis of cells expressing high *gfp* showed that the *Ins2*(GFP)^{HIGH} cells had significant alterations in genes involved in hormone regulation, hormone secretion, hormone transport, protein synthesis, and protein cleavage (Fig. 6D). Cluster of genes ordered by correlation with *gfp* in heterozygous *Ins2*$^{GFP/WT}$ β cells showed that *Sema6a,* and the antioxidant metalothionein genes *Mt1* and *Mt2*, were most closely correlated to *gfp* mRNA at the single cell level. Classical genes related to β cell function and maturity that were positively correlated with *gfp* include *Ins2, Ero1lb,* Chromagranin A (*Chga*), the Glut2 glucose transporter *Slc2a2, Iapp, Nkx6-1,* and *Pdx1* (Augsornworawat et al., 2021; Benner et al., 2014; Zito et al., 2010). The *gfp*-high state was also characterized by increased mRNA expression of genes encoding signal recognition particle 9 (*Srp9*), G-protein subunit gamma 12 (*Gng12*), nucleotide pyrophosphatase/phosphodiesterase 2 (*Enpp2*), aldehyde dehydrogenase 5 family member A1 (*Aldh5a1*), and tetraspanin-28 (*Cd81*). Stress response genes, such as *Sec61b*, *Sec61g* and *Sec23b* were also highly expressed(Sundaram et al., 2017; Yehia et al., 2021). The *gfp*-high state was associated with decreased expression of genes including soluble factors such as peptide YY (*Pyy*), somatostatin *(Sst)*, glucagon (*Gcg*) pancreatic polypeptide (*Ppy*), suggesting in aggregate a less 'poly-hormonal' and therefore, more mature, gene expression profile (Basford et al., 2012; Hrvatin et al., 2014; Johnson, 2016). In agreement with this, *gfp*-high β cells had lower expression of pappalysin 2 (*Pappa2*), an α cell-selective regulator of insulin-like growth factor bioavailability, and the epsilon cell marker (*Etv1*) (Segerstolpe et al., 2016)(Fig. 6E). *Gfp*-high cells also had reduced expression of several genes linked to insulin production and secretion, such as multiple subunits of the 40S and 60S ribosomes, eukaryotic translation initiation factor 3 subunit C (*Eif3c*), Eukaryotic translation initiation factor 2 subunit 2 (*Eif2s2*), and heat shock 70kDa protein 9 (*Hspa9;* Mortalin)(Fig. 6E). Interestingly, a decrease in the expression of certain ER stress genes was found, including *Prkcsh*, *Nucb2*, and *Fam129a* (Evstafieva et al., 2018; Shin et al., 2019; Zhang et al., 2018). Thus, in young mice, the *Ins2*(GFP)^{HIGH} cell state is associated with a mature single cell gene expression profile, optimal insulin secretion and a reorganization of protein synthesis machinery.

Age is known to significantly alter the properties of pancreatic β cells, including their function and ability to enter the cell cycle (Rankin and Kushner, 2009). Thus, we conducted an additional similar study in three 60 week-old mice. In this experiment, we studied cells from both *Ins2*$^{GFP/WT}$ (Fig. 7A-E) and *Ins2*$^{GFP/GFP}$ islets (Supplemental Fig. S, 7, 8, 9). Cluster analysis of genes ordered by *gfp* gradient in old heterozygous *Ins2*$^{GFP/WT}$ β cells revealed that *Ins2* expression most closely matches *gfp* mRNA (Fig. 7E). Similar to the younger mice, genes that increased with *gfp* expression included genes related to optimal insulin secretion such as chromogranin A (*Chga*) and the Glut2 glucose transporter (*Slc2a2*), as well as key β cell transcription factors and maturity markers *Nkx6-1* and *Pdx1*. Other genes related to insulin production and secretion that were upregulated include *Ins1*, secretogranin 3 (*Scg3*), proprotein convertase subtilisin/kexin type 1 (*Pcsk1*), ubiquinol-cytochrome c reductase complex assembly factor 2 (*Uqcc2*), synaptotagmin-like 4 (*Sytl4*) (Cambier et al., 2012; Lin et al., 2019; Szabat *et al.*, 2012). There was also an enrichment in key β cell transcription factors and maturity markers *Ucn3* and *Neurod1* (Blum et al., 2012; Fu et al., 2013*)*. Interestingly, many of the mRNAs that were increased are known to be *Pdx1* target genes in islets (Sachdeva et al., 2009). Other notable genes that were upregulated in *gfp*-high cells were G-protein subunit gamma 12 (*Gng12)*, protein phosphatase 1 regulatory inhibitor subunit 1A (*Ppp1r1a*), nucleotide pyrophosphatase/phosphodiesterase 2 (*Enpp2*), and metabolism-regulating genes, such as glucose-6-phosphatase catalytic subunit 2 (*G6pc2*) and hydroxyacyl-CoA dehydrogenase (*Hadh*) (Fig. 7E). ER stress-related gene *Neat1* was also increased (Adriaens et al., 2016). Also in agreement with the analysis of young islets, *gfp*-high β cells from old homozygous mice had decreased expression of *Pappa2*, *Etv1*, and *Sst*, as well as other markers of β cell immaturity (*Gcg*, *Ppy*, *Pyy*). *Ldha*, another de-differentiation marker, was also negatively correlated with *gfp*. Several ER stress genes were also anti-correlated with *gfp*, including *Eef2* and *Spp1(Boyce et al., 2008; Lepine et al., 2011)*. Thus, in older mice, the *Ins2*(GFP)^{HIGH} cell state is overall similar to younger mice, with a more mature single cell expression profile and association with genes related to insulin secretion.

Separately, we analyzed genes ordered by *gfp* mRNA gradient in old homozygous *Ins2*$^{GFP/GFP}$ β cells (Supplemental Fig. S8). Many of the same genes that we observed in the heterozygous samples were also increased in the GFP homozygous samples, including *Chga*, *Neurod1*, *Pdx1*, *Ucn3*, *Slc2a2*, *Gng12*, and *Ppp1r1a*. Genes that were anti-correlated with *gfp* mRNA old homozygous *Ins2*$^{GFP/GFP}$ β cells include multiple genes found in the heterozygous samples (Fig. 7), such as de-differentiation markers (*Sst*, *Pyy, Ppy, Gcg*). Nuclear protein 1, transcriptional regulator (*Nupr1)*, a stress adaptation gene, was reduced in homozygous *Ins2*$^{GFP/GFP}$ β cells with high *gfp* expression. When we combined data from *Ins2*$^{GFP/WT}$ and *Ins2*$^{GFP/GFP}$ cells, pathway enrichment analysis of high *gfp*-expressing cells in older mice showed that the *Ins2*(GFP)^{HIGH} cells had significant alterations in genes involved in protein translation, RNA splicing, mRNA processing (Fig. 7D). With this combined analysis, *gfp* correlation with many of the same genes found by analysing *Ins2*$^{GFP/WT}$ and *Ins2*$^{GFP/GFP}$ cells separately were also identified (Supplemental Fig. S9). Pathway enrichment analysis of differential expression in *Ins1* positive cells revealed upregulation in genes related to translation machinery in younger mice, while in older mice there was upregulation in genes related to cellular respiration (Supplemental Fig. S10).

The single cell RNA sequencing studies identified enrichment in genes that control β cell stress responses and markers of β cell maturity. We have previously shown that insulin production itself is a significant stress under basal conditions in β cells (Szabat *et al.*, 2016) and we therefore predicted that cells with increased *Ins2* gene activity and GFP production would be more sensitive to stress. Indeed, *Ins2*(GFP)^{HIGH} cells were >10 fold more sensitive to apoptosis at all glucose concentrations we tested when compared with *Ins2*(GFP)^{LOW} cells in the same cultures (Fig. 6A). Thus, the states marked by high gene activity at the endogenous *Ins2* locus are likely to possess critical functional differences.

Discussion

The goal of the present study was to determine the nature of *Ins2* gene expression heterogeneity. Analysis of pancreatic tissue sections from *Ins2*^{GFP} knock-in mice showed that, at any given time, roughly 40% of all β cells exist in a GFP-high state, suggesting that not all β cells have simultaneously high levels of active transcription at the *Ins2* locus *in vivo*. Over the course of multi-day *in vitro* imaging

experiments, we observed clear transitions between *Ins2*(GFP)^{HIGH} and *Ins2*(GFP)^{LOW} states in single β cells, possibly linked to the circadian clock. However, *Ins2* gene activity was stable for the duration of these studies in the majority of cells. We used single cell RNA sequencing to characterize the *Ins2*(GFP)^{HIGH} cellular state and found that *Ins2*(GFP)^{HIGH} were significantly more sensitive under all stress conditions examined. Together with previous live cell imaging data, the results of the present study demonstrate that a substantial component of β cell heterogeneity is dynamic in time (Fig. 8B).

The dynamics of GFP fluorescence revealed by live cell imaging of dispersed islet cells from *Ins2*^{GFP} mice provided an unprecedented look at insulin gene activity in populations of single β cells. Many of the *Ins2*(GFP)^{LOW} and *Ins2*(GFP)^{HIGH} β cell states were maintained over at least 24 hours. Autocorrelation analysis showed that of the cells which displayed at least one oscillation, a significant proportion have oscillation periods clustered at 8-12 hours. Circadian control of islet function is essential for maintaining normal glucose homeostasis, and circadian-based variations on the transcriptional level have been described in diverse cell types and shown to be critical for optimization of cellular function (Kalsbeek et al., 2014; Saini et al., 2016). Insulin is both a target of circadian regulation, and a regulator of the circadian machinery in many cell types (Allaman-Pillet et al., 2004; Ohta et al., 2017; Perelis et al., 2015; Rakshit et al., 2015; Ribas-Latre and Eckel-Mahan, 2016; Tahara and Shibata, 2018). Diurnal rhythms of β cell function and metabolism has long been recognized (Groop and Harno, 1980; Polonsky et al., 1988), and our study extends this to activity at the insulin gene locus.

The study of pancreatic islet cell heterogeneity is currently experiencing resurgence, in part due to the application of single cell sequencing and optogenetic technologies to answer islet biology questions. There are many examples of β cell heterogeneity and these were reviewed recently (Benninger and Hodson, 2018). Insulin gene expression is a cardinal feature of pancreatic β cells, but cell-by cell variability in insulin production has remained under-appreciated despite published evidence (Kiekens *et al.*, 1992). For example, there are reports of significant β cell heterogeneity in transgenic mice expressing GFP under the *Ins2* promoter (Katsuta et al., 2012). Similarly, we have shown variation in fluorescent protein expression under the control of *Ins1* promoters *in vivo* and *in vitro* (Szabat *et al.*, 2010; Szabat *et al.*, 2009; Szabat *et al.*, 2011). However, a limitation in these studies is that artificial promoter constructs may not recapitulate the more complex and long-range regulation available at the endogenous gene locus. Notwithstanding, cell-by cell analysis of insulin mRNA, either by single-molecule fluorescent *in situ* hybridization or single cell RNA sequencing, also showed a 2- to 10-fold range in native gene expression from endogenous insulin gene loci (Farack *et al.*, 2019; Xin *et al.*, 2018). The *Ins2*(GFP)^{HIGH} β cells we identified in our study are likely to be the temporal manifestation of the extreme β cells reported by Farack et al. Supporting this, and consistent with our single cell RNA sequencing data, their extreme β cells had significantly elevated *Chga, Pdx1, Slc2a2,* and *Ucn3* mRNA expression (Farack *et al.*, 2019). It is also notable that both extreme β cells and our *Ins2*(GFP)^{HIGH} β cells had relatively normal total insulin staining, a clue that further supports the transient nature of dynamics in endogenous *Ins2* gene activity. It is possible that the dynamic nature of insulin transcription is an adaptation to the extremely high demands of producing and maintaining adequate stores of insulin in β cells. Assuming there are homeostatic mechanisms to maintain stable insulin protein stores, it is unclear how the need for a burst of insulin gene activity would be sensed by individual β cells. Future studies should attempt to define these mechanisms.

The relationship between β cell states demarked by insulin expression and disease pathogenesis remains unclear. Type 1 diabetes risk is associated with an increase in *INS* mRNA in whole human fetal pancreas (Vafiadis et al., 1996) and single adult β cells pancreas (Wang et al., 2020). Isolated islets and single human β cells from people with type 2 diabetes were reported to have reduced *INS* expression on average (Segerstolpe *et al.*, 2016; Yang et al., 2011), although our recent meta-analysis of single cell RNA sequencing data sets did not find a statistically significant reduction in INS mRNA levels in β-cells from donors with type 2 diabetes (Wang *et al.*, 2020). Extreme β cells were significantly more common in diabetic *db*/*db* mice (Farack *et al.*, 2019). We found that the *Ins2*(GFP)^{HIGH} state was associated with significant vulnerability to cellular stress, so having an excess number of *Ins2*(GFP)^{HIGH} β cells at a given time may negatively affect islet health and robustness. These results are consistent with our previous data defining the interrelationships between maximal insulin production, ER stress

and β cell proliferation (Szabat *et al.*, 2016). It is also likely that stress may modulate the frequency of β cell state transitions, although we did not test this directly. The presence of a proportion of β cells in the *Ins2*(GFP)^{LOW} state may also be essential for islet function. Specifically, so called 'hub β cells' that help synchronize islets were reported to have lower insulin content compared with typical β cells (Johnston *et al.*, 2016), and we have speculated that this represents a trade-off needed for their synchronizing function (Kolic and Johnson, 2016). Rodent and human β cells are long-lived (Perl et al., 2010; Teta et al., 2005), and perhaps β cells cycle through multiple states during their existence, including taking turns supporting the oscillatory coupling of the islet. Given that robust β cell heterogeneity and state transitions have not been reported for stem cell derived β-like cells (Veres et al., 2019), it is likely that *in vitro* differentiation protocols will need to be further optimized to produce a full range of dynamic β cell characteristics. Interestingly, many of the genes that are differentially expressed in *Ins2*(GFP)^{HIGH} β cells are known to play roles in type 2 diabetes susceptibility, including common alleles of the MODY/neonatal diabetes genes *Pdx1*, *Neurod1*, *Nkx6.1*, *Abcc8*, *Slc2a2*, as well as *Slc30a8* and *Pam* genome-wide association previously identified by genome-wide association (Thomsen et al., 2018). It will also be interesting to examine the frequency of β cell states in the context of type 1 diabetes, given that pro-insulin, *Pdx1*, *Iapp*, and *Chga* are auto-antigens (Han et al., 2013; Nakayama et al., 2005; Stadinski et al., 2010). Indeed, β cells undergoing proliferation or with lower insulin/maturity are protected in the NOD mouse model of type 1 diabetes (Dirice et al., 2019; Rui et al., 2017). Collectively, these observations suggest that modulation of β cell states could be a therapeutic and/or prevention target for both type 1 diabetes and type 2 diabetes.

Temporal transcriptional plasticity and gene expression bursting on a similar time scale as to what we have observed have been documented in bacteria, yeast and other mammalian cell types (Raj et al., 2006; Suter et al., 2011; Vera et al., 2016). For example, bursting gene expression patterns have been observed in pituitary cells (Harper et al., 2010; Norris et al., 2003; Walsh and Shupnik, 2009). Interestingly, LHβ transcription in pituitary gonadotrophs is directly linked to proteasome activity (Walsh and Shupnik, 2009), suggesting a possible mechanism for coupling protein loads and transcription in secretory cell types. Many cell-extrinsic and cell-intrinsic factors have been implicated in the modulation of transcriptional burst frequency, including histone modifications and chromatin topology(Atger et al., 2015; Molina et al., 2013; Nicolas et al., 2017; Nicolas et al., 2018; Phillips et al., 2019). Future studies will be required to determine the molecular mechanisms mediating transcriptional bursting at the insulin gene locus in β cells. Future studies should also seek to directly measure *Ins2* mRNA transcription, perhaps using new CRISPR-based probes or other mRNA tagging systems (Pichon et al., 2018; Pichon et al., 2020; Vera et al., 2019).

In this study, we identified a subpopulation of cells which had relatively rapid transitions between *Ins2*(GFP)^{LOW} and *Ins2*(GFP)^{HIGH} β cell states. This suggests dynamic transcriptional activity at the *Ins2* gene locus rather than stable heterogeneity. However, our study has several limitations. For example, our measurements of GFP fluorescence originating from the *Ins2* locus-mediated transcription cannot distinguish the relative contribution in changes in GFP mRNA transcription/stability or GFP protein translation/degradation. The half-life of unmodified GFP is ~26 hours (Corish and Tyler-Smith, 1999) and the changes in GFP fluorescence in some cells suggest coordinated increases of protein synthesis and coupled protein degradation. Long term imaging also causes extensive photo-bleaching, which may be the reason we observed a general decrease of GFP fluorescence over time, which we attempted to correct with de-trending techniques. While some intercellular signals could be missing in our analysis of dispersed islet cells (Chowdhury et al., 2013; Scarl et al., 2019), our *in vivo* analysis revealed a similar proportion of *Ins2*(GFP)^{LOW} and *Ins2*(GFP)^{HIGH} giving us confidence that the phenomenon we measured *in vitro* is generalizable to *in vivo* conditions. Future experiments should involve more powerful live cell imaging techniques, including tissue slides and intraviral imaging, ideally with techniques that allow long-term cell tracking without excess phototoxicity or photo-bleaching (Kiepas et al., 2020; Laissue et al., 2017).

In conclusion, our data demonstrate that single β cells can switch between states marked by high and low activity of the phylogenetically conserved, endogenous insulin gene locus. This newly discovered phenomenon may account for much of the observed β cell heterogeneity measured at single

time points and needs to be comprehensively studied and leveraged in efforts to protect β cells in the context of diabetes and to generate new β cells from stem cells (Alvarez-Dominguez et al., 2020; Johnson, 2016).

Methods

Animals and in vivo physiology

Animals were housed and studied in the Modified Barrier Facility using protocols approved by the UBC Animal Care Committee in accordance with international guidelines. *Ins2*$^{GFP/WT}$ knock-in mice were obtained from Shouhong Xuan (Wakae-Takada *et al.*, 2013). These mice were crossed with transgenic mice where the *Ins1* promoter drives a mCherry:H2B fluorescent fusion protein (Benner *et al.*, 2014). Glucose tolerance and insulin secretion were assessed in both male and female mice (12-14 weeks) injected intraperitoneally with 2g/kg (20%) glucose after a 5 hr fast. Insulin from *in vivo* samples was measured using ELISA kits from Alpco (Salem, NH, USA). Insulin tolerance was assessed after injection of 0.75 U insulin per kg body weight after a 5 hr fast.

Immunostaining

Pancreata from PBS perfused mice were harvested and fixed in 4% paraformaldehyde for 24 hr before being washed and stored in 70% ethanol, prior to paraffin embedding. Pancreatic sections (5 µm) were taken from at least three different regions of the pancreas 100 µm apart. Sections were deparaffinized, hydrated with decreasing concentrations of ethanol, and rinsed with PBS. Sections were subjected to 15 min of heat-induced epitope retrieval at 95°C using a 10 mM citrate buffer, pH 6.0. Sections were blocked then incubated with primary antibodies overnight in a humid chamber at 4°C. A list of primary antibodies can be found in Antibodies section. Primary antibodies were visualized following incubation with secondary antibodies conjugated to AlexaFluor 488, 555, 594, or 647 as required (1:1,000; Invitrogen). Counter staining was done by Vectasheild mounting media with DAPI (H-1200). Images for β cell and α cell area were taken on ImageXpress^{MICRO} using a 10× (NA 0.3) objective and analyzed using the MetaXpress software (Molecular Devices Corporation, San Jose, CA, USA). All other images were taken on a Zeiss 200M microscope using 20× air (NA 0.75), 40× oil (NA 1.3), and/or 100× oil (NA 1.45) objectives and analyzed using Slidebook software (Intelligent Imaging Innovations, Denver, CO, USA). For quantification of immunofluorescence, we used the segment masking function of Slidebook, generating a GFP high mask and a GFP low mask (by subtracting the GFP high mask from the insulin mask). A list of primary antibodies can be found in Table S1.

Islet isolation and culture

Pancreatic islets were isolated using collagenase, filtration, and hand-picking as described (Szabat et al., 2010). Islets were cultured overnight (37°C, 5% CO_2) in RPMI1640 medium (Invitrogen) with 11 mM glucose (Sigma), 100 units/ml penicillin, 100 µg/ml streptomycin (Invitrogen), and 10% vol/vol FBS (Invitrogen). Real-time RT-PCR was conducted as described previously (Szabat *et al.*, 2016). A list of primers used can be found in Table S2.

For experiments involving various culture conditions, cells were incubated overnight in serum-free media for serum-free and serum-starved conditions, and media with 10% FBS for serum conditions. Prior to imaging, cells were given a media change and stained with Hoechst cell nuclei marker and propidium iodide cell death marker for 2 hours. Serum-free condition cells were given media with no serum, while serum-starved (rescue) and serum conditions were given media with 10% FBS. Cells were then treated with various glucose concentrations immediately prior to imaging.

Fluorescence-activated cell sorting

Pancreatic islets were dispersed using 0.005% trypsin and resuspended in 1xPBS with 0.005% FBS. Dispersed islets were then filtered into 5 ml polypropylene tubes. Fluorescence-activated cell sorting was conducted on a Cytopeia Influx sorter (Becton Dickinson, Franklin Lakes, NJ, USA) at the Life Sciences Institute core facility. Cells were excited with a 488 nm laser (530/40 emission) and a 561 nm laser (610/20 emission).

Live cell imaging

To define the incidence and kinetics of the transitions in *Ins2* gene activity, we cultured dispersed islet cells on 96-well glass bottom plates, and imaged them every 5 or 30 minutes for up to 96 hours through a 40x air objective using a ImageXpress^{MICRO} environmentally-controlled, robotic imaging system (Molecular Devices)(Yang and Johnson, 2013).

Imaging of human β cells stained for insulin and *Pdx1* was done using methods described previously (Szabat *et al.*, 2009)

Image analysis

Analysis of *Ins2*^{GFP}:*Ins1*-mCherry cells was done using ImageXpress software and custom R scripts (Matthews et al., 1983). Hierarchical clustering with 8 cellular behavior traits as features was done, and a heatmap was constructed using the pheatmap function. Traits were calculated using R functions and formulas, including mean (average life time fluorscent intensity), sharp (calculates number of sharp peaks in a cell's lifetime), AUC (area under curve), FWHM (full width at half maximum), oscillation (mean average deviation). Principle component analysis was done using the same 8 cellular behavior traits as variables. We performed model-based clustering using the mclust function in R, and projected the cells onto the first two principle components.

Analysis of *Ins2*^{GFP} cells was done using MetaXpress analysis software and custom R scripts. Hierarchical clustering was done with various cellular behavior traits as features, and a heatmap was constructed using the pheatmap function in R. Features include ACF time (calculates when the autocorrelation function equals 0 in a time series), FWHM (full width at half maximum), difference (calculates the range of fluorescent intensity change), deviation (mean average deviation), mean (average lifetime relative fluorescent intensity), and sharp (a function which detects sharp peaks). Principle component analysis was done using the same cellular behavior traits as variables. We performed K-means clustering using the kmeans function in R, and projected the cells onto the first two principle components.

De-trending and normalizing were done by comparing various treatments to the basal (10 mM glucose) and normalizing to the average fluorescence intensity of first 2 hours of imaging to correct for a linear photobleaching artifact and variations in the initial hours of imaging.

Autocorrelation analysis

Autocorrelation analysis of single mutant *Ins2*$^{GFP/WT}$ was done using the acf function in R (Chen et al., 1987). To calculate the oscillation periods of GFP, we first selected for cells with at least one oscillation. We calculated the autocorrelation function of all cells for all time-points, and filtered for cells with at least two significantly positive peaks (autocorrelation function >0.1) using a find peaks function in R (Matthews *et al.*, 1983), indicating an oscillation. We calculated oscillation periods by finding the distance of the two positive peaks to get a full wavelength period. Oscillation periods of oscillating cells with more than one oscillation were then binned in 4-hour intervals and plotted into a barchart using R scripts.

Live cell imaging of cell death

Our methods for live cell imaging of islet cell survival have been previously published (Yang and Johnson, 2013). Briefly, pancreatic islet cells were dissociated, and cultured in RPMI 1640 media with 10% FBS (Gibco, Fisher Scientific, Gaithersburg, MD, USA), and penicillin/streptomycin on 96 well glass bottom plates for 48 hours. Dispersed islet cells were then exposed to different dose of glucose, as well as thapsigargin (Sigma, St. Louis, MO, USA). Islet cell death was measured by propidium iodide incorporation. Images were taken every 30 min for up to 48 hours, as described earlier. Propidium iodide incorporation was traced throughout the time period, and area under the curve was measured.

Single cell transcriptomics

Single Cell Suspension was loaded on the 10x genomics single cell controller for capture in droplet emulsion. The 60-week old mouse islet cell libraries were prepared using the Chromium Single Cell 3' Reagent v2 Chemistry kit (10x Genomics, Pleasanton, CA, USA) and the standard protocol was

followed for all steps. The 8-week old mouse islet cell libraries were prepared using the Chromium Single Cell 3' Reagent v3 Chemistry kit (10x Genomics). Libraries were then sequenced on a Nextseq500 (Illumina). Cell Ranger 3.0 (10x Genomics) was used to process raw fastq data. The results were visualized using 10x Genomics Loupe Cell Browser. Cells with high mitochondria gene ratios (>0.1), low numbers of genes (<500), and low UMI counts (<1000) were excluded prior to analysis. This was done for both 60-week-old mouse data and 8-week-old mouse data respectively.

Seurat R package (version 4.0.4) was used to perform analysis. (Butler et al., 2018). Data was normalized, scaled and analyzed with PCA. PCs generated were used to build a UMAP, with which we used to identify populations of cells using known cellular markers (*Ins1* for β cells, *Gcg* for α-cells, *Sst* for δ cells, *Ppy* for pancreatic polypeptide/ γ cells, *Ghrl* for ε cells, and *Pcam1* for endothelial cells). Cells that had high *Ins1* reads were selected, and the rest were used as a base expression level for differential expression analysis using the *FindMarker*s function in Seurat. Differential expression analysis between different subsets of cells was performed using the Wilcoxon rank sum test option in Seurat. Differential expression analysis over GFP gradient was performed by first calculating correlation functions for each gene with GFP, then selecting for the genes which had the highest values. Top hits were used for pathway enrichment analyses and heatmaps. Pathway enrichment analysis was performed using custom R scripts with data from Gene Ontology Resource database.

Statistical analysis

Data are shown as mean plus/minus standard error of the mean unless otherwise indicated. Differences between 2 groups were evaluated with Student's t-test and between more than 2 groups using ANOVA and Kruskal–Wallis one-way analysis of variance, calculated with custom R-scripts and Prizm software (Graphpad Software, San Diego, CA, USA).

References

Adriaens, C., Standaert, L., Barra, J., Latil, M., Verfaillie, A., Kalev, P., Boeckx, B., Wijnhoven, P.W., Radaelli, E., Vermi, W., et al. (2016). p53 induces formation of NEAT1 lncRNA-containing paraspeckles that modulate replication stress response and chemosensitivity. Nat Med *22*, 861-868. 10.1038/nm.4135.

Allaman-Pillet, N., Roduit, R., Oberson, A., Abdelli, S., Ruiz, J., Beckmann, J.S., Schorderet, D.F., and Bonny, C. (2004). Circadian regulation of islet genes involved in insulin production and secretion. Mol Cell Endocrinol *226*, 59-66. 10.1016/j.mce.2004.06.001.

Alvarez-Dominguez, J.R., Donaghey, J., Rasouli, N., Kenty, J.H.R., Helman, A., Charlton, J., Straubhaar, J.R., Meissner, A., and Melton, D.A. (2020). Circadian Entrainment Triggers Maturation of Human In Vitro Islets. Cell Stem Cell *26*, 108-122 e110. 10.1016/j.stem.2019.11.011.

Atger, F., Gobet, C., Marquis, J., Martin, E., Wang, J., Weger, B., Lefebvre, G., Descombes, P., Naef, F., and Gachon, F. (2015). Circadian and feeding rhythms differentially affect rhythmic mRNA transcription and translation in mouse liver. Proc Natl Acad Sci U S A *112*, E6579-6588. 10.1073/pnas.1515308112.

Augsornworawat, P., Maxwell, K.G., Velazco-Cruz, L., and Millman, J.R. (2021). Single-cell transcriptome profiling reveals beta cell maturation in stem cell-derived islets after transplantation. Cell Rep *34*, 108850. 10.1016/j.celrep.2021.108850.

Bader, E., Migliorini, A., Gegg, M., Moruzzi, N., Gerdes, J., Roscioni, S.S., Bakhti, M., Brandl, E., Irmler, M., Beckers, J., et al. (2016). Identification of proliferative and mature beta-cells in the islets of Langerhans. Nature *535*, 430-434. 10.1038/nature18624.

Basford, C.L., Prentice, K.J., Hardy, A.B., Sarangi, F., Micallef, S.J., Li, X., Guo, Q., Elefanty, A.G., Stanley, E.G., Keller, G., et al. (2012). The functional and molecular characterisation of human embryonic stem cell-derived insulin-positive cells compared with adult pancreatic beta cells. Diabetologia *55*, 358-371. 10.1007/s00125-011-2335-x.

Benner, C., van der Meulen, T., Caceres, E., Tigyi, K., Donaldson, C.J., and Huising, M.O. (2014). The transcriptional landscape of mouse beta cells compared to human beta cells reveals notable species

differences in long non-coding RNA and protein-coding gene expression. BMC Genomics *15*, 620. 10.1186/1471-2164-15-620.
Benninger, R.K.P., and Hodson, D.J. (2018). New Understanding of beta-Cell Heterogeneity and In Situ Islet Function. Diabetes *67*, 537-547. 10.2337/dbi17-0040.
Blum, B., Hrvatin, S., Schuetz, C., Bonal, C., Rezania, A., and Melton, D.A. (2012). Functional beta-cell maturation is marked by an increased glucose threshold and by expression of urocortin 3. Nat Biotechnol *30*, 261-264. 10.1038/nbt.2141.
Boland, B.B., Rhodes, C.J., and Grimsby, J.S. (2017). The dynamic plasticity of insulin production in beta-cells. Mol Metab *6*, 958-973. 10.1016/j.molmet.2017.04.010.
Boyce, M., Py, B.F., Ryazanov, A.G., Minden, J.S., Long, K., Ma, D., and Yuan, J. (2008). A pharmacoproteomic approach implicates eukaryotic elongation factor 2 kinase in ER stress-induced cell death. Cell Death Differ *15*, 589-599. 10.1038/sj.cdd.4402296.
Butler, A., Hoffman, P., Smibert, P., Papalexi, E., and Satija, R. (2018). Integrating single-cell transcriptomic data across different conditions, technologies, and species. Nat Biotechnol *36*, 411-420. 10.1038/nbt.4096.
Cambier, L., Rassam, P., Chabi, B., Mezghenna, K., Gross, R., Eveno, E., Auffray, C., Wrutniak-Cabello, C., Lajoix, A.D., and Pomies, P. (2012). M19 modulates skeletal muscle differentiation and insulin secretion in pancreatic beta-cells through modulation of respiratory chain activity. PLoS One *7*, e31815. 10.1371/journal.pone.0031815.
Chen, S., Thakor, N.V., and Mower, M.M. (1987). Ventricular fibrillation detection by a regression test on the autocorrelation function. Med Biol Eng Comput *25*, 241-249. 10.1007/BF02447420.
Chowdhury, A., Dyachok, O., Tengholm, A., Sandler, S., and Bergsten, P. (2013). Functional differences between aggregated and dispersed insulin-producing cells. Diabetologia *56*, 1557-1568. 10.1007/s00125-013-2903-3.
Corish, P., and Tyler-Smith, C. (1999). Attenuation of green fluorescent protein half-life in mammalian cells. Protein Eng *12*, 1035-1040.
Dirice, E., Kahraman, S., De Jesus, D.F., El Ouaamari, A., Basile, G., Baker, R.L., Yigit, B., Piehowski, P.D., Kim, M.J., Dwyer, A.J., et al. (2019). Increased β-cell proliferation before immune cell invasion prevents progression of type 1 diabetes. Nature Metabolism.
Dorrell, C., Schug, J., Canaday, P.S., Russ, H.A., Tarlow, B.D., Grompe, M.T., Horton, T., Hebrok, M., Streeter, P.R., Kaestner, K.H., and Grompe, M. (2016). Human islets contain four distinct subtypes of beta cells. Nat Commun *7*, 11756. 10.1038/ncomms11756.
Evans-Molina, C., Garmey, J.C., Ketchum, R., Brayman, K.L., Deng, S., and Mirmira, R.G. (2007). Glucose regulation of insulin gene transcription and pre-mRNA processing in human islets. Diabetes *56*, 827-835. 10.2337/db06-1440.
Evstafieva, A.G., Kovaleva, I.E., Shoshinova, M.S., Budanov, A.V., and Chumakov, P.M. (2018). Implication of KRT16, FAM129A and HKDC1 genes as ATF4 regulated components of the integrated stress response. PLoS One *13*, e0191107. 10.1371/journal.pone.0191107.
Farack, L., Golan, M., Egozi, A., Dezorella, N., Bahar Halpern, K., Ben-Moshe, S., Garzilli, I., Toth, B., Roitman, L., Krizhanovsky, V., and Itzkovitz, S. (2019). Transcriptional Heterogeneity of Beta Cells in the Intact Pancreas. Dev Cell *48*, 115-125 e114. 10.1016/j.devcel.2018.11.001.
Fu, Z., Gilbert, E.R., and Liu, D. (2013). Regulation of insulin synthesis and secretion and pancreatic Beta-cell dysfunction in diabetes. Curr Diabetes Rev *9*, 25-53.
Groop, L., and Harno, K. (1980). Diurnal pattern of plasma insulin and blood glucose during glibenclamide and glipizide therapy in elderly diabetics. Acta Endocrinol Suppl (Copenh) *239*, 44-52.
Han, S., Donelan, W., Wang, H., Reeves, W., and Yang, L.J. (2013). Novel autoantigens in type 1 diabetes. Am J Transl Res *5*, 379-392.
Harper, C.V., Featherstone, K., Semprini, S., Friedrichsen, S., McNeilly, J., Paszek, P., Spiller, D.G., McNeilly, A.S., Mullins, J.J., Davis, J.R., and White, M.R. (2010). Dynamic organisation of prolactin gene expression in living pituitary tissue. J Cell Sci *123*, 424-430. 10.1242/jcs.060434.
Heimberg, H., De Vos, A., Vandercammen, A., Van Schaftingen, E., Pipeleers, D., and Schuit, F. (1993). Heterogeneity in glucose sensitivity among pancreatic beta-cells is correlated to differences in glucose phosphorylation rather than glucose transport. Embo J *12*, 2873-2879.

Hrvatin, S., O'Donnell, C.W., Deng, F., Millman, J.R., Pagliuca, F.W., DiIorio, P., Rezania, A., Gifford, D.K., and Melton, D.A. (2014). Differentiated human stem cells resemble fetal, not adult, beta cells. Proc Natl Acad Sci U S A *111*, 3038-3043. 10.1073/pnas.1400709111.
Johnson, J.D. (2016). The quest to make fully functional human pancreatic beta-cells from embryonic stem cells: Climbing a mountain in the clouds. Diabetologia *59*, 2047-2057. 10.1007/s00125-016-4059-4.
Johnson, J.D., Ahmed, N.T., Luciani, D.S., Han, Z., Tran, H., Fujita, J., Misler, S., Edlund, H., and Polonsky, K.S. (2003). Increased islet apoptosis in Pdx1+/- mice. J Clin Invest *111*, 1147-1160. 10.1172/JCI16537.
Johnson, J.D., Bernal-Mizrachi, E., Alejandro, E.U., Han, Z., Kalynyak, T.B., Li, H., Beith, J.L., Gross, J., Warnock, G.L., Townsend, R.R., et al. (2006). Insulin protects islets from apoptosis via Pdx1 and specific changes in the human islet proteome. Proc Natl Acad Sci U S A *103*, 19575-19580. 10.1073/pnas.0604208103.
Johnston, N.R., Mitchell, R.K., Haythorne, E., Pessoa, M.P., Semplici, F., Ferrer, J., Piemonti, L., Marchetti, P., Bugliani, M., Bosco, D., et al. (2016). Beta Cell Hubs Dictate Pancreatic Islet Responses to Glucose. Cell Metab *24*, 389-401. 10.1016/j.cmet.2016.06.020.
Kalsbeek, A., la Fleur, S., and Fliers, E. (2014). Circadian control of glucose metabolism. Mol Metab *3*, 372-383. 10.1016/j.molmet.2014.03.002.
Katsuta, H., Aguayo-Mazzucato, C., Katsuta, R., Akashi, T., Hollister-Lock, J., Sharma, A.J., Bonner-Weir, S., and Weir, G.C. (2012). Subpopulations of GFP-marked mouse pancreatic beta-cells differ in size, granularity, and insulin secretion. Endocrinology *153*, 5180-5187. 10.1210/en.2012-1257.
Kiekens, R., In 't Veld, P., Mahler, T., Schuit, F., Van De Winkel, M., and Pipeleers, D. (1992). Differences in glucose recognition by individual rat pancreatic B cells are associated with intercellular differences in glucose-induced biosynthetic activity. J Clin Invest *89*, 117-125. 10.1172/JCI115551.
Kiepas, A., Voorand, E., Mubaid, F., Siegel, P.M., and Brown, C.M. (2020). Optimizing live-cell fluorescence imaging conditions to minimize phototoxicity. J Cell Sci *133*. 10.1242/jcs.242834.
Knoch, K.P., Nath-Sain, S., Petzold, A., Schneider, H., Beck, M., Wegbrod, C., Sonmez, A., Munster, C., Friedrich, A., Roivainen, M., and Solimena, M. (2014). PTBP1 is required for glucose-stimulated cap-independent translation of insulin granule proteins and Coxsackieviruses in beta cells. Mol Metab *3*, 518-530. 10.1016/j.molmet.2014.05.002.
Kolic, J., and Johnson, J.D. (2016). Specialized Hub Beta Cells Trade Maximal Insulin Production for Perfect Timing. Cell Metab *24*, 371-373. 10.1016/j.cmet.2016.08.022.
Laissue, P.P., Alghamdi, R.A., Tomancak, P., Reynaud, E.G., and Shroff, H. (2017). Assessing phototoxicity in live fluorescence imaging. Nat Methods *14*, 657-661. 10.1038/nmeth.4344.
Lepine, S., Allegood, J.C., Park, M., Dent, P., Milstien, S., and Spiegel, S. (2011). Sphingosine-1-phosphate phosphohydrolase-1 regulates ER stress-induced autophagy. Cell Death Differ *18*, 350-361. 10.1038/cdd.2010.104.
Leroux, L., Desbois, P., Lamotte, L., Duvillie, B., Cordonnier, N., Jackerott, M., Jami, J., Bucchini, D., and Joshi, R.L. (2001). Compensatory responses in mice carrying a null mutation for Ins1 or Ins2. Diabetes *50 Suppl 1*, S150-153. 10.2337/diabetes.50.2007.s150.
Lin, C.C., Cheng, K.P., Hung, H.C., Li, C.H., Lin, C.H., Chang, C.J., Hu, C.Y., Wu, H.T., and Ou, H.Y. (2019). Serum Secretogranin III Concentrations Were Increased in Subjects with Metabolic Syndrome and Independently Associated with Fasting Plasma Glucose Levels. J Clin Med *8*. 10.3390/jcm8091436.
Ling, Z., Chen, M.C., Smismans, A., Pavlovic, D., Schuit, F., Eizirik, D.L., and Pipeleers, D.G. (1998). Intercellular differences in interleukin 1beta-induced suppression of insulin synthesis and stimulation of noninsulin protein synthesis by rat pancreatic beta-cells. Endocrinology *139*, 1540-1545.
Matthews, D.R., Lang, D.A., Burnett, M.A., and Turner, R.C. (1983). Control of pulsatile insulin secretion in man. Diabetologia *24*, 231-237. 10.1007/BF00282705.
Mehran, A.E., Templeman, N.M., Brigidi, G.S., Lim, G.E., Chu, K.Y., Hu, X., Botezelli, J.D., Asadi, A., Hoffman, B.G., Kieffer, T.J., et al. (2012). Hyperinsulinemia drives diet-induced obesity independently of brain insulin production. Cell Metab *16*, 723-737. 10.1016/j.cmet.2012.10.019.

Molina, N., Suter, D.M., Cannavo, R., Zoller, B., Gotic, I., and Naef, F. (2013). Stimulus-induced modulation of transcriptional bursting in a single mammalian gene. Proc Natl Acad Sci U S A *110*, 20563-20568. 10.1073/pnas.1312310110.
Nakayama, M., Abiru, N., Moriyama, H., Babaya, N., Liu, E., Miao, D., Yu, L., Wegmann, D.R., Hutton, J.C., Elliott, J.F., and Eisenbarth, G.S. (2005). Prime role for an insulin epitope in the development of type 1 diabetes in NOD mice. Nature *435*, 220-223. 10.1038/nature03523.
Nicolas, D., Phillips, N.E., and Naef, F. (2017). What shapes eukaryotic transcriptional bursting? Mol Biosyst *13*, 1280-1290. 10.1039/c7mb00154a.
Nicolas, D., Zoller, B., Suter, D.M., and Naef, F. (2018). Modulation of transcriptional burst frequency by histone acetylation. Proc Natl Acad Sci U S A *115*, 7153-7158. 10.1073/pnas.1722330115.
Norris, A.J., Stirland, J.A., McFerran, D.W., Seymour, Z.C., Spiller, D.G., Loudon, A.S., White, M.R., and Davis, J.R. (2003). Dynamic patterns of growth hormone gene transcription in individual living pituitary cells. Mol Endocrinol *17*, 193-202. 10.1210/me.2002-0201.
Ohta, Y., Taguchi, A., Matsumura, T., Nakabayashi, H., Akiyama, M., Yamamoto, K., Fujimoto, R., Suetomi, R., Yanai, A., Shinoda, K., and Tanizawa, Y. (2017). Clock Gene Dysregulation Induced by Chronic ER Stress Disrupts beta-cell Function. EBioMedicine *18*, 146-156. 10.1016/j.ebiom.2017.03.040.
Perelis, M., Marcheva, B., Ramsey, K.M., Schipma, M.J., Hutchison, A.L., Taguchi, A., Peek, C.B., Hong, H., Huang, W., Omura, C., et al. (2015). Pancreatic beta cell enhancers regulate rhythmic transcription of genes controlling insulin secretion. Science *350*, aac4250. 10.1126/science.aac4250.
Perl, S., Kushner, J.A., Buchholz, B.A., Meeker, A.K., Stein, G.M., Hsieh, M., Kirby, M., Pechhold, S., Liu, E.H., Harlan, D.M., and Tisdale, J.F. (2010). Significant human beta-cell turnover is limited to the first three decades of life as determined by in vivo thymidine analog incorporation and radiocarbon dating. J Clin Endocrinol Metab *95*, E234-239. 10.1210/jc.2010-0932.
Phillips, N.E., Mandic, A., Omidi, S., Naef, F., and Suter, D.M. (2019). Memory and relatedness of transcriptional activity in mammalian cell lineages. Nat Commun *10*, 1208. 10.1038/s41467-019-09189-8.
Pichon, X., Lagha, M., Mueller, F., and Bertrand, E. (2018). A Growing Toolbox to Image Gene Expression in Single Cells: Sensitive Approaches for Demanding Challenges. Mol Cell *71*, 468-480. 10.1016/j.molcel.2018.07.022.
Pichon, X., Robert, M.C., Bertrand, E., Singer, R.H., and Tutucci, E. (2020). New Generations of MS2 Variants and MCP Fusions to Detect Single mRNAs in Living Eukaryotic Cells. Methods Mol Biol *2166*, 121-144. 10.1007/978-1-0716-0712-1_7.
Pipeleers, D.G. (1992). Heterogeneity in pancreatic beta-cell population. Diabetes *41*, 777-781. 10.2337/diab.41.7.777.
Polonsky, K.S., Given, B.D., and Van Cauter, E. (1988). Twenty-four-hour profiles and pulsatile patterns of insulin secretion in normal and obese subjects. J Clin Invest *81*, 442-448. 10.1172/JCI113339.
Raj, A., Peskin, C.S., Tranchina, D., Vargas, D.Y., and Tyagi, S. (2006). Stochastic mRNA synthesis in mammalian cells. PLoS Biol *4*, e309. 10.1371/journal.pbio.0040309.
Rakshit, K., Qian, J., Colwell, C.S., and Matveyenko, A.V. (2015). The islet circadian clock: entrainment mechanisms, function and role in glucose homeostasis. Diabetes Obes Metab *17 Suppl 1*, 115-122. 10.1111/dom.12523.
Rankin, M.M., and Kushner, J.A. (2009). Adaptive beta-cell proliferation is severely restricted with advanced age. Diabetes *58*, 1365-1372. 10.2337/db08-1198.
Ribas-Latre, A., and Eckel-Mahan, K. (2016). Interdependence of nutrient metabolism and the circadian clock system: Importance for metabolic health. Mol Metab *5*, 133-152. 10.1016/j.molmet.2015.12.006.
Rui, J., Deng, S., Arazi, A., Perdigoto, A.L., Liu, Z., and Herold, K.C. (2017). beta Cells that Resist Immunological Attack Develop during Progression of Autoimmune Diabetes in NOD Mice. Cell Metab *25*, 727-738. 10.1016/j.cmet.2017.01.005.
Sachdeva, M.M., Claiborn, K.C., Khoo, C., Yang, J., Groff, D.N., Mirmira, R.G., and Stoffers, D.A. (2009). Pdx1 (MODY4) regulates pancreatic beta cell susceptibility to ER stress. Proc Natl Acad Sci U S A *106*, 19090-19095. 10.1073/pnas.0904849106.

Saini, C., Petrenko, V., Pulimeno, P., Giovannoni, L., Berney, T., Hebrok, M., Howald, C., Dermitzakis, E.T., and Dibner, C. (2016). A functional circadian clock is required for proper insulin secretion by human pancreatic islet cells. Diabetes Obes Metab *18*, 355-365. 10.1111/dom.12616.
Scarl, R.T., Corbin, K.L., Vann, N.W., Smith, H.M., Satin, L.S., Sherman, A., and Nunemaker, C.S. (2019). Intact pancreatic islets and dispersed beta-cells both generate intracellular calcium oscillations but differ in their responsiveness to glucose. Cell Calcium *83*, 102081. 10.1016/j.ceca.2019.102081.
Segerstolpe, A., Palasantza, A., Eliasson, P., Andersson, E.M., Andreasson, A.C., Sun, X., Picelli, S., Sabirsh, A., Clausen, M., Bjursell, M.K., et al. (2016). Single-Cell Transcriptome Profiling of Human Pancreatic Islets in Health and Type 2 Diabetes. Cell Metab *24*, 593-607. 10.1016/j.cmet.2016.08.020.
Shin, G.C., Moon, S.U., Kang, H.S., Choi, H.S., Han, H.D., and Kim, K.H. (2019). PRKCSH contributes to tumorigenesis by selective boosting of IRE1 signaling pathway. Nat Commun *10*, 3185. 10.1038/s41467-019-11019-w.
Stadinski, B.D., Delong, T., Reisdorph, N., Reisdorph, R., Powell, R.L., Armstrong, M., Piganelli, J.D., Barbour, G., Bradley, B., Crawford, F., et al. (2010). Chromogranin A is an autoantigen in type 1 diabetes. Nat Immunol *11*, 225-231. 10.1038/ni.1844.
Sundaram, A., Plumb, R., Appathurai, S., and Mariappan, M. (2017). The Sec61 translocon limits IRE1alpha signaling during the unfolded protein response. Elife *6*. 10.7554/eLife.27187.
Suter, D.M., Molina, N., Gatfield, D., Schneider, K., Schibler, U., and Naef, F. (2011). Mammalian genes are transcribed with widely different bursting kinetics. Science *332*, 472-474. 10.1126/science.1198817.
Szabat, M., Johnson, J.D., and Piret, J.M. (2010). Reciprocal modulation of adult beta cell maturity by activin A and follistatin. Diabetologia *53*, 1680-1689. 10.1007/s00125-010-1758-0.
Szabat, M., Luciani, D.S., Piret, J.M., and Johnson, J.D. (2009). Maturation of adult beta-cells revealed using a Pdx1/insulin dual-reporter lentivirus. Endocrinology *150*, 1627-1635. 10.1210/en.2008-1224.
Szabat, M., Lynn, F.C., Hoffman, B.G., Kieffer, T.J., Allan, D.W., and Johnson, J.D. (2012). Maintenance of beta-cell maturity and plasticity in the adult pancreas: developmental biology concepts in adult physiology. Diabetes *61*, 1365-1371. 10.2337/db11-1361.
Szabat, M., Page, M.M., Panzhinskiy, E., Skovso, S., Mojibian, M., Fernandez-Tajes, J., Bruin, J.E., Bround, M.J., Lee, J.T., Xu, E.E., et al. (2016). Reduced Insulin Production Relieves Endoplasmic Reticulum Stress and Induces beta Cell Proliferation. Cell Metab *23*, 179-193. 10.1016/j.cmet.2015.10.016.
Szabat, M., Pourghaderi, P., Soukhatcheva, G., Verchere, C.B., Warnock, G.L., Piret, J.M., and Johnson, J.D. (2011). Kinetics and genomic profiling of adult human and mouse beta-cell maturation. Islets *3*, 175-187. 10.4161/isl.3.4.15881.
Tahara, Y., and Shibata, S. (2018). Entrainment of the mouse circadian clock: Effects of stress, exercise, and nutrition. Free Radic Biol Med *119*, 129-138. 10.1016/j.freeradbiomed.2017.12.026.
Teta, M., Long, S.Y., Wartschow, L.M., Rankin, M.M., and Kushner, J.A. (2005). Very slow turnover of beta-cells in aged adult mice. Diabetes *54*, 2557-2567.
Thomsen, S.K., Raimondo, A., Hastoy, B., Sengupta, S., Dai, X.Q., Bautista, A., Censin, J., Payne, A.J., Umapathysivam, M.M., Spigelman, A.F., et al. (2018). Type 2 diabetes risk alleles in PAM impact insulin release from human pancreatic beta-cells. Nat Genet *50*, 1122-1131. 10.1038/s41588-018-0173-1.
Tillmar, L., Carlsson, C., and Welsh, N. (2002). Control of insulin mRNA stability in rat pancreatic islets. Regulatory role of a 3'-untranslated region pyrimidine-rich sequence. J Biol Chem *277*, 1099-1106. 10.1074/jbc.M108340200.
Vafiadis, P., Bennett, S.T., Colle, E., Grabs, R., Goodyer, C.G., and Polychronakos, C. (1996). Imprinted and genotype-specific expression of genes at the IDDM2 locus in pancreas and leucocytes. J Autoimmun *9*, 397-403. 10.1006/jaut.1996.0054.
van der Meulen, T., Mawla, A.M., DiGruccio, M.R., Adams, M.W., Nies, V., Dolleman, S., Liu, S., Ackermann, A.M., Caceres, E., Hunter, A.E., et al. (2017). Virgin Beta Cells Persist throughout Life at a Neogenic Niche within Pancreatic Islets. Cell Metab *25*, 911-926 e916. 10.1016/j.cmet.2017.03.017.
Vera, M., Biswas, J., Senecal, A., Singer, R.H., and Park, H.Y. (2016). Single-Cell and Single-Molecule Analysis of Gene Expression Regulation. Annual review of genetics *50*, 267-291. 10.1146/annurev-genet-120215-034854.

Vera, M., Tutucci, E., and Singer, R.H. (2019). Imaging Single mRNA Molecules in Mammalian Cells Using an Optimized MS2-MCP System. Methods Mol Biol *2038*, 3-20. 10.1007/978-1-4939-9674-2_1.
Veres, A., Faust, A.L., Bushnell, H.L., Engquist, E.N., Kenty, J.H., Harb, G., Poh, Y.C., Sintov, E., Gurtler, M., Pagliuca, F.W., et al. (2019). Charting cellular identity during human in vitro beta-cell differentiation. Nature *569*, 368-373. 10.1038/s41586-019-1168-5.
Wakae-Takada, N., Xuan, S., Watanabe, K., Meda, P., and Leibel, R.L. (2013). Molecular basis for the regulation of islet beta cell mass in mice: the role of E-cadherin. Diabetologia *56*, 856-866. 10.1007/s00125-012-2824-6.
Walsh, H.E., and Shupnik, M.A. (2009). Proteasome regulation of dynamic transcription factor occupancy on the GnRH-stimulated luteinizing hormone beta-subunit promoter. Mol Endocrinol *23*, 237-250. 10.1210/me.2008-0098.
Wang, S., Flibotte, S., Camunas-Soler, J., MacDonald, P.E., and Johnson, J.D. (2020). The type 1 diabetes at-risk allele at rs3842753 associates with increased beta cell INS mRNA in a meta-analysis of single cell RNA sequencing data. bioRxiv, 2020.2012.2006.413971. 10.1101/2020.12.06.413971.
Wang, S., Flibotte, S., Camunas-Soler, J., MacDonald, P.E., and Johnson, J.D. (2021). A New Hypothesis for Type 1 Diabetes Risk: The At-Risk Allele at rs3842753 Associates With Increased Beta-cell INS Messenger RNA in a Meta-Analysis of Single-Cell RNA-Sequencing Data. Can J Diabetes. 10.1016/j.jcjd.2021.03.007.
Wills, Q.F., Boothe, T., Asadi, A., Ao, Z., Warnock, G.L., Kieffer, T.J., and Johnson, J.D. (2016). Statistical approaches and software for clustering islet cell functional heterogeneity. Islets *8*, 48-56. 10.1080/19382014.2016.1150664.
Xin, Y., Dominguez Gutierrez, G., Okamoto, H., Kim, J., Lee, A.H., Adler, C., Ni, M., Yancopoulos, G.D., Murphy, A.J., and Gromada, J. (2018). Pseudotime Ordering of Single Human beta-Cells Reveals States of Insulin Production and Unfolded Protein Response. Diabetes *67*, 1783-1794. 10.2337/db18-0365.
Yang, B.T., Dayeh, T.A., Kirkpatrick, C.L., Taneera, J., Kumar, R., Groop, L., Wollheim, C.B., Nitert, M.D., and Ling, C. (2011). Insulin promoter DNA methylation correlates negatively with insulin gene expression and positively with HbA(1c) levels in human pancreatic islets. Diabetologia *54*, 360-367. 10.1007/s00125-010-1967-6.
Yang, Y.H., and Johnson, J.D. (2013). Multi-parameter single-cell kinetic analysis reveals multiple modes of cell death in primary pancreatic beta-cells. J Cell Sci *126*, 4286-4295. 10.1242/jcs.133017.
Yehia, L., Liu, D., Fu, S., Iyer, P., and Eng, C. (2021). Non-canonical role of wild-type SEC23B in the cellular stress response pathway. Cell Death Dis *12*, 304. 10.1038/s41419-021-03589-9.
Zhang, D., Lin, J., Chao, Y., Zhang, L., Jin, L., Li, N., He, R., Ma, B., Zhao, W., and Han, C. (2018). Regulation of the adaptation to ER stress by KLF4 facilitates melanoma cell metastasis via upregulating NUCB2 expression. J Exp Clin Cancer Res *37*, 176. 10.1186/s13046-018-0842-z.
Zito, E., Chin, K.T., Blais, J., Harding, H.P., and Ron, D. (2010). ERO1-beta, a pancreas-specific disulfide oxidase, promotes insulin biogenesis and glucose homeostasis. J Cell Biol *188*, 821-832. 10.1083/jcb.200911086.

Figure Legends

Figure 1. *In vivo* heterogeneity of insulin content and gene activity in human and mouse islets. **(A)** Variability in insulin and PDX1 protein levels in human pancreatic β cells *in vivo*. Scale bar is 20 μm. **(B)** The *Ins2*$^{GFP/GFP}$ knock-in mouse model. Illustration shows, with scale, the replacement of most of the second exon with wildtype GFP. The wildtype *Ins2* locus is shown for comparison, including RNA-seq exon coverage, aggregate (filtered) from NCBI *Mus musculus* Annotation release 106 (log 2 base scaled). **(C)** Normal glucose homeostasis in *Ins2*$^{GFP/WT}$;*Ins2*$^{GFP/GFP}$ mice and WT (Male n=4-8, Female

n=3-44-5). **(D)** GFP from the endogenous *Ins2* gene locus is high in a subset of mouse pancreatic β cells. Scale bar is 20 μm. **(E)** Detection of *Ins2*(GFP)^{LOW} and *Ins2*(GFP)^{HIGH} populations of β cells by FACS. (**F**) Presumed transcription-to-maturation times of GFP and insulin. See Supplemental Information for calculations and references.

Figure 2. Tracking β cell heterogeneity with *Ins1*-mCherry;*Ins2*$^{GFP/WT}$ knock-in mice. (A) Experimental model for tracking activity at the endogenous *Ins2* locus (GFP) in β cells marked with mCherry driven by an *Ins1* promoter, which constitutively marks 98% of β cells. Scale bar is 50 μm. **(B)** Live cell imaging of islet cells isolated and dispersed from *Ins1*-mCherry;*Ins2*$^{GFP/WT}$ mice. Scale bar is 50 μm. **(C,D)** Distinct populations of *Ins2*(GFP)^{LOW} β cells and *Ins2*(GFP)^{HIGH} β cells were FACS purified and examined by qPCR for *gfp*, *Ins2*, and *Ins1* mRNA (n=3 mice). Units are relative expression calculated from ΔCT, then normalized to wild-type. One-way analysis of variance. **(E)** Dynamic imaging, over 30 hours in culture, of dispersed islet cells from *Ins1*-mCherry;*Ins2*$^{GFP/WT}$ mice labelled with Hoechst vital nuclear dye. Note the examples of cells with bursting GFP fluorescence. Scale bar is 50 μm. * $p < 0.05$, ** $p < 0.01$, *** $p < 0.001$

Figure 3. Live cell imaging *Ins2* gene activity reveals bursting behavior of the endogenous *Ins2* gene locus. (A) Dynamic imaging, of up to 96 hours in culture, of dispersed islet cells from *Ins2*$^{GFP/WT}$ mice. Cells were labelled with Hoechst vital nuclear dye and propidium iodide cell death marker. Note the examples of cells with fluctuating GFP fluorescence. Changes in cell distribution in the red and blue wavelength can be attributed to deceased cells detaching from the bottom of the well. Scale bar is 40 μm. **(B)** Segmentation of cells for analysis. Cells with 100 relative fluorescent intensity compared to background were selected, comprising of ~70% of all cells imaged. Scale bar is 40 μm. **(C)** Examples of cells with dynamics in relative fluorescent intensity over time. Units are relative fluorescent intensity to background. **(D)** Lifetime average GFP fluorescence of all cells imaged. Units are relative fluorescent intensity to background. **(E)** Clustering of cellular dynamics of *Ins2* gene activity (GFP), Hoechst vital nuclear dye, and propidium iodide cell death marker. Hierarchical clustering of 6 parameters calculated from intensity over time of the green wavelength. Parameters include deviation (mean average deviation), FWHM (full width at half maximum), mean (lifetime average GFP intensity), ACF time (function which calculates when the autocorrelation function equals 0 in a time series), difference (maximum value minus minimum value) and sharp (counts number of sharp peaks in a cell's lifetime).

Figure 4. Autocorrelation analysis of cells with fluctuating behavior reveals possible connections to circadian rhythm. (A) Ratio of cells at least one and no oscillations. Autocorrelation functions of cells across all time-points were calculated, and oscillation detection was done using a findpeaks function in R. For line plots, units are relative fluorescent intensity to background. For autocorrelagrams, units are autocorrelation function, calculated with the acf function in R. **(B)** Traits of oscillating cells. Average life-time GFP fluorescence intensity relative to background of oscillating versus non-oscillating cells and bar-chart of cell oscillation periods binned in 4-hour intervals. Only cells with at least one oscillation were plotted (357 out of 2115 cells), and oscillation periods were calculated by finding the distance between two peaks in autocorrelograms. Student's T-test. * $p < 0.05$, ** $p < 0.01$, *** $p < 0.001$

Figure 5. Effects of media glucose concentration on *Ins2* gene activity. (A) Changes in GFP fluorescence over time. Calculated by normalizing to first two hours of imaging to remove initial variation, followed by de-trending to control for photobleaching. AUC was calculated using this modified data. **(B)** Quantification and comparison of raw GFP fluorescence and ratios of oscillating versus non-oscillating cells at the 48-hour mark across all treatments. Units are relative fluorescent intensity to background. Kruskal–Wallis one-way analysis of variance**.** * $p < 0.05$, ** $p < 0.01$, *** $p < 0.001$

Figure 6. Single cell RNA sequencing analysis of *Ins2*(GFP)^{LOW} and *Ins2*(GFP)^{HIGH} β cells in young mice. (A) UMAP plot of all cells isolated and dispersed from *Ins2*$^{GFP/WT}$ mice and FACS purified into either GFP-negative (-) or GFP-positive (+) groups. **(B)** UMAPs with known markers for major cell

populations in islets. Cells were selected for analysis based on high *Ins1* expression and low expression of other cell population markers. **(C)** Log-normalized counts of *Ins1, Ins2,* and *gfp* mRNA quantification distributions from GFP-negative or GFP-positive single β cells. **(D)** Gene Ontology Categories that are driven by genes differentially expressed in *Ins2*(GFP)^{LOW} versus *Ins2*(GFP)^{HIGH} β cells. **(E)** Individual genes that are differentially expressed as a function of *gfp* mRNA expression.

Figure 6. Single cell RNA sequencing analysis of *Ins2*(GFP)^{LOW} and *Ins2*(GFP)^{HIGH} β cells in old mice. (A) UMAP plot of all isolated and dispersed from *Ins2*$^{GFP/WT}$ or *Ins2*$^{GFP/GFP}$ mice and FACS purified into either GFP-negative (-) or GFP-positive (+) groups. **(B)** UMAPs with known markers for major cell populations in islets. Cells were selected for analysis based on high *Ins1* expression and low expression of other cell population markers. **(C)** Log-normalized counts of *Ins1, Ins2,* and *gfp* mRNA quantification distributions from GFP-negative or GFP-positive single β cells. **(D)** Gene Ontology categories that are driven by genes differentially expressed in *Ins2*(GFP)^{LOW} versus *Ins2*(GFP)^{HIGH} β cells. **(E)** Individual genes that are differentially expressed as a function of *gfp* mRNA expression.

Figure 7. *Ins2*(GFP)^{HIGH} β cells show increased cell death across multiple conditions. (A) Cells with high GFP intensities show increased apoptosis susceptibility at all tested glucose concentrations and in the presence of thapsigargin (>1000 cells/condition, repeated from 2 mice). **(B)** Hypothetical working model of transitions between insulin production states in β cells.

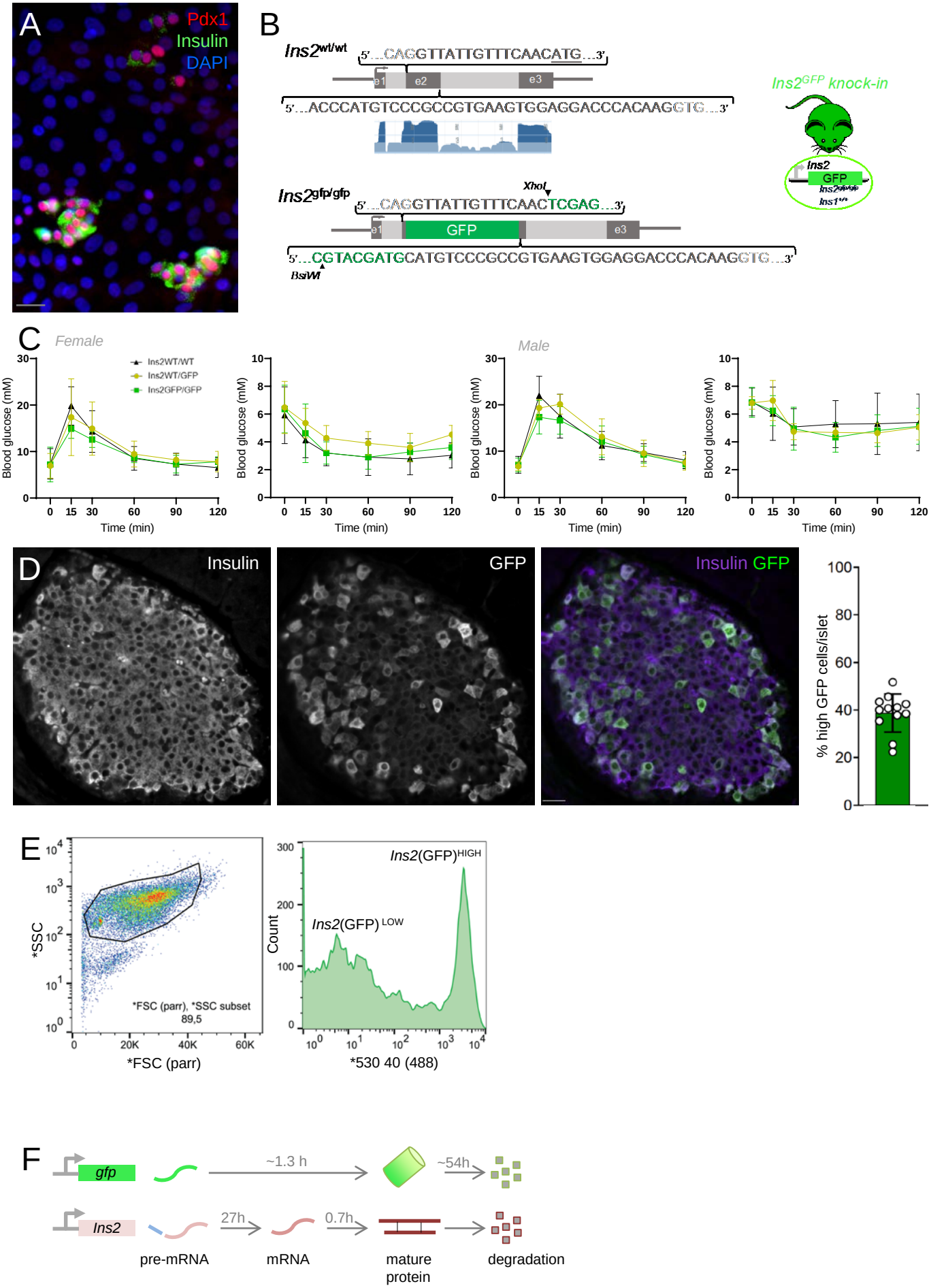
A
Pdx1
Insulin
DAPI
B
Ins2wt/wt
5'...CAGGTTATTGTTTCAACATG...3'
e1
e2
e3
5'...ACCCATGTCCCGCCGTGAAGTGGAGGACCCACAAGGTG...3'
Ins2GFP knock-in
Ins2
GFP
Ins2gfp/gfp
Ins1wt/wt
Ins2gfp/gfp
XhoI
5'...CAGGTTATTGTTTCAACTCGAG...3'
GFP
5'...CGTACGATGCATGTCCCGCCGTGAAGTGGAGGACCCACAAGGTG...3'
BsiWI
C
Female
Male
Ins2WT/WT
Ins2WT/GFP
Ins2GFP/GFP
Blood glucose (mM)
Time (min)
D
Insulin
GFP
Insulin GFP
% high GFP cells/islet
E
*SSC
*FSC (parr)
*FSC (parr), *SSC subset
89,5
Count
Ins2(GFP)HIGH
Ins2(GFP) LOW
*530 40 (488)
F
gfp
~1.3 h
~54h
Ins2
27h
0.7h
pre-mRNA
mRNA
mature protein
degradation

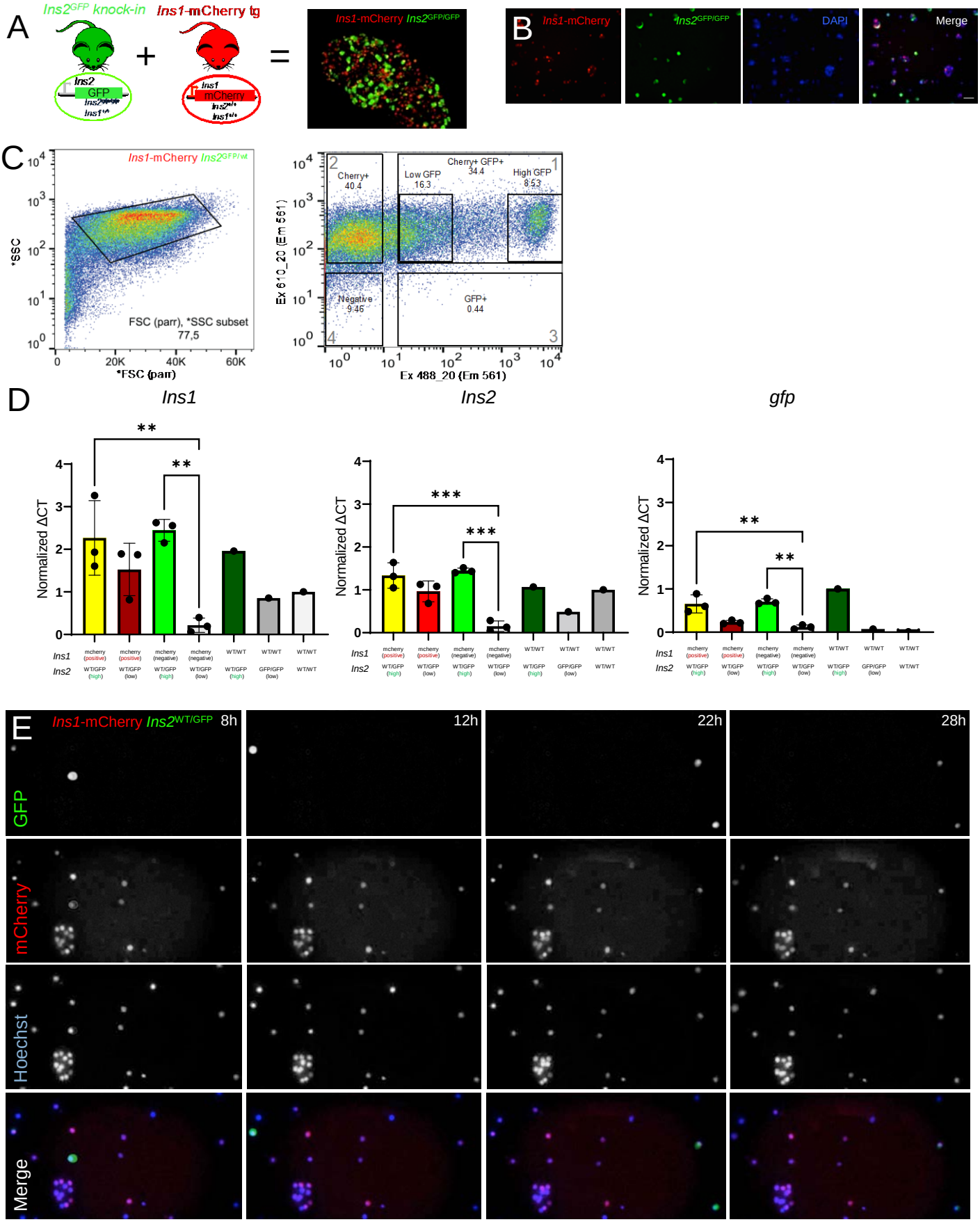
A
Ins2GFP knock-in
Ins1-mCherry tg
Ins2
GFP
Ins1
mCherry
Ins1-mCherry Ins2GFP/GFP
B
Ins1-mCherry
Ins2GFP/GFP
DAPI
Merge
C
Ins1-mCherry Ins2GFP/wt
*SSC
*FSC (parr)
FSC (parr), *SSC subset
77,5
Cherry+
40.4
Low GFP
16.3
Cherry+ GFP+
34.4
High GFP
8.53
Negative
9.46
GFP+
0.44
Ex 610_20 (Em 561)
Ex 488_20 (Em 561)
D
Ins1
Ins2
gfp
Normalized ΔCT
Ins1
Ins2
E
Ins1-mCherry Ins2WT/GFP
8h
12h
22h
28h
GFP
mCherry
Hoechst
Merge

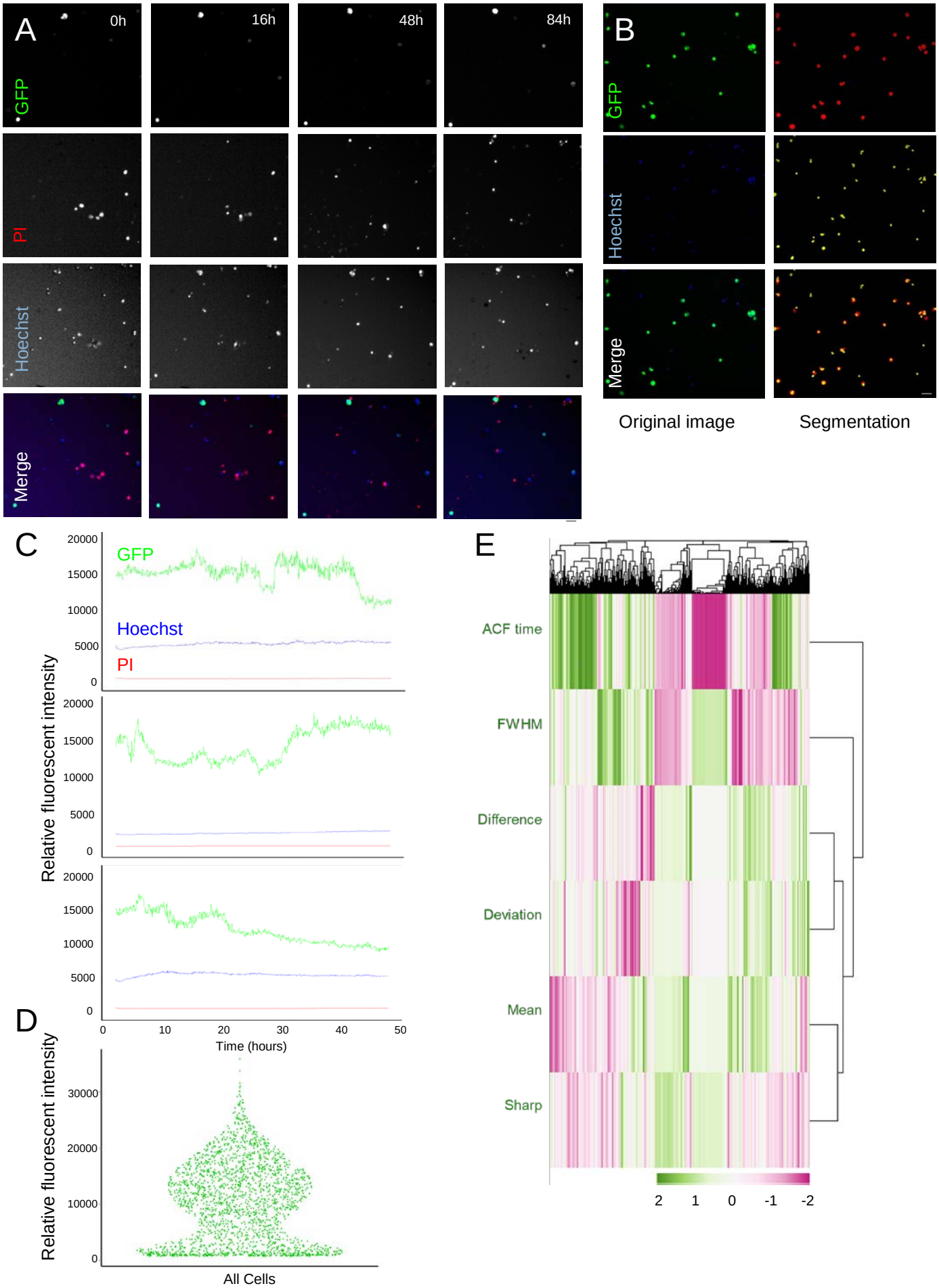
A
0h
16h
48h
84h
GFP
PI
Hoechst
Merge
B
GFP
Hoechst
Merge
Original image
Segmentation
C
GFP
Hoechst
PI
Relative fluorescent intensity
20000
15000
10000
5000
0
0
10
20
30
40
50
Time (hours)
D
Relative fluorescent intensity
30000
20000
10000
0
All Cells
E
ACF time
FWHM
Difference
Deviation
Mean
Sharp
2
1
0
-1
-2

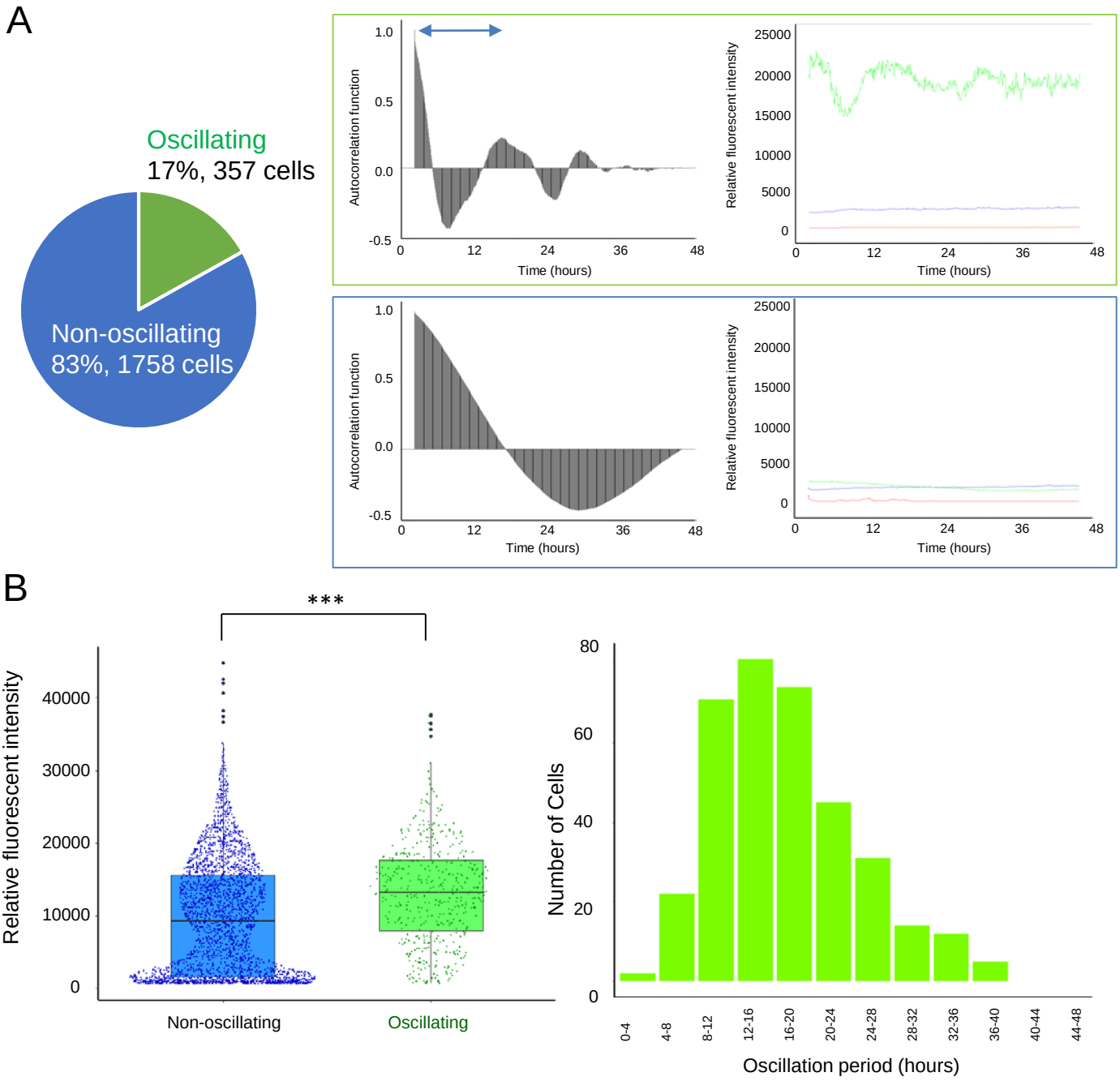
A
Oscillating
17%, 357 cells
Non-oscillating
83%, 1758 cells
Autocorrelation function
Time (hours)
Relative fluorescent intensity
B
***
Relative fluorescent intensity
Non-oscillating
Oscillating
Number of Cells
Oscillation period (hours)
0-4
4-8
8-12
12-16
16-20
20-24
24-28
28-32
32-36
36-40
40-44
44-48

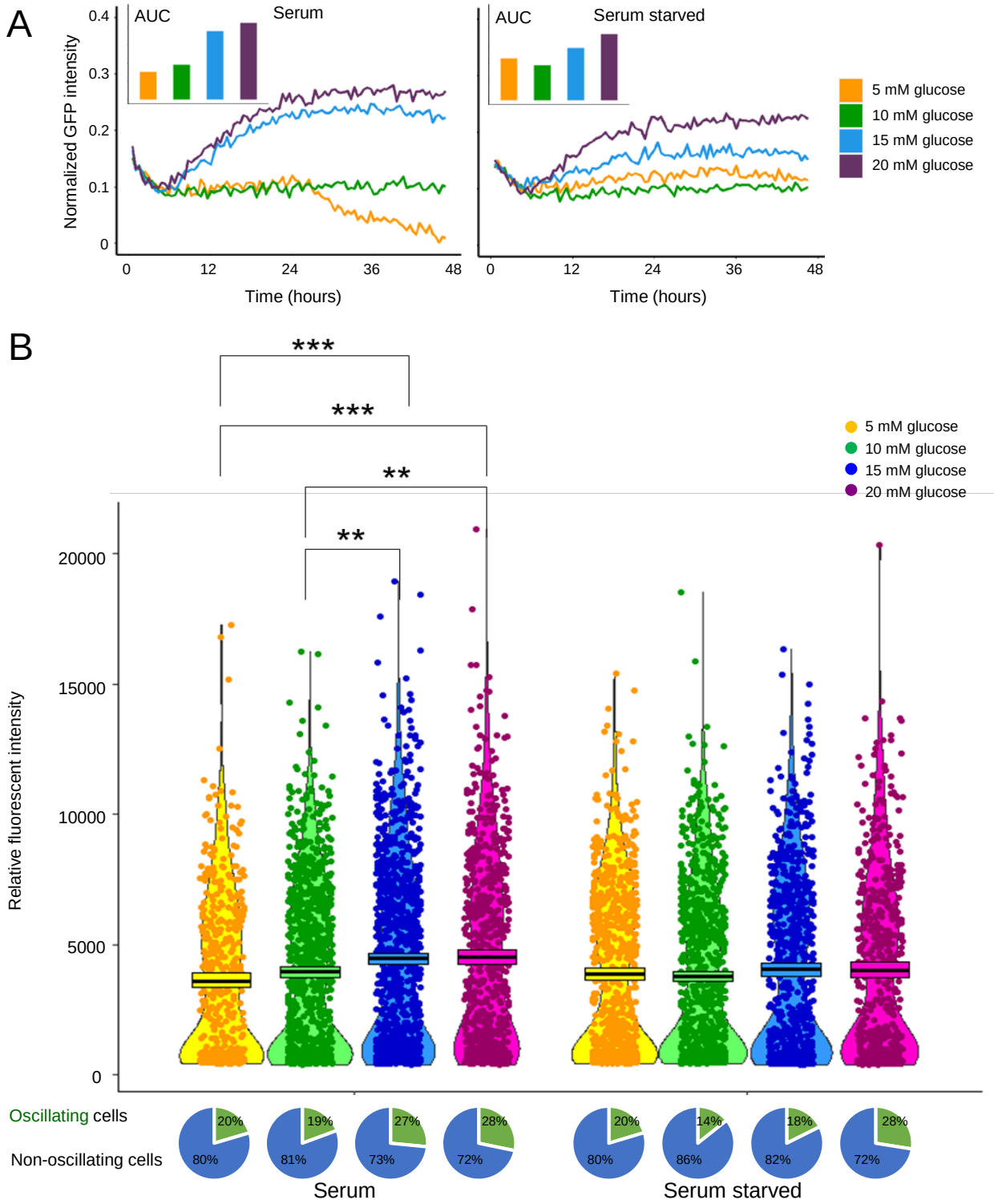
A
AUC
Serum
AUC
Serum starved
Normalized GFP intensity
0.4
0.3
0.2
0.1
0
0
12
24
36
48
Time (hours)
5 mM glucose
10 mM glucose
15 mM glucose
20 mM glucose
B
***
***
**
**
5 mM glucose
10 mM glucose
15 mM glucose
20 mM glucose
Relative fluorescent intensity
20000
15000
10000
5000
0
Oscillating cells
Non-oscillating cells
20%
80%
19%
81%
27%
73%
28%
72%
20%
80%
14%
86%
18%
82%
28%
72%
Serum
Serum starved

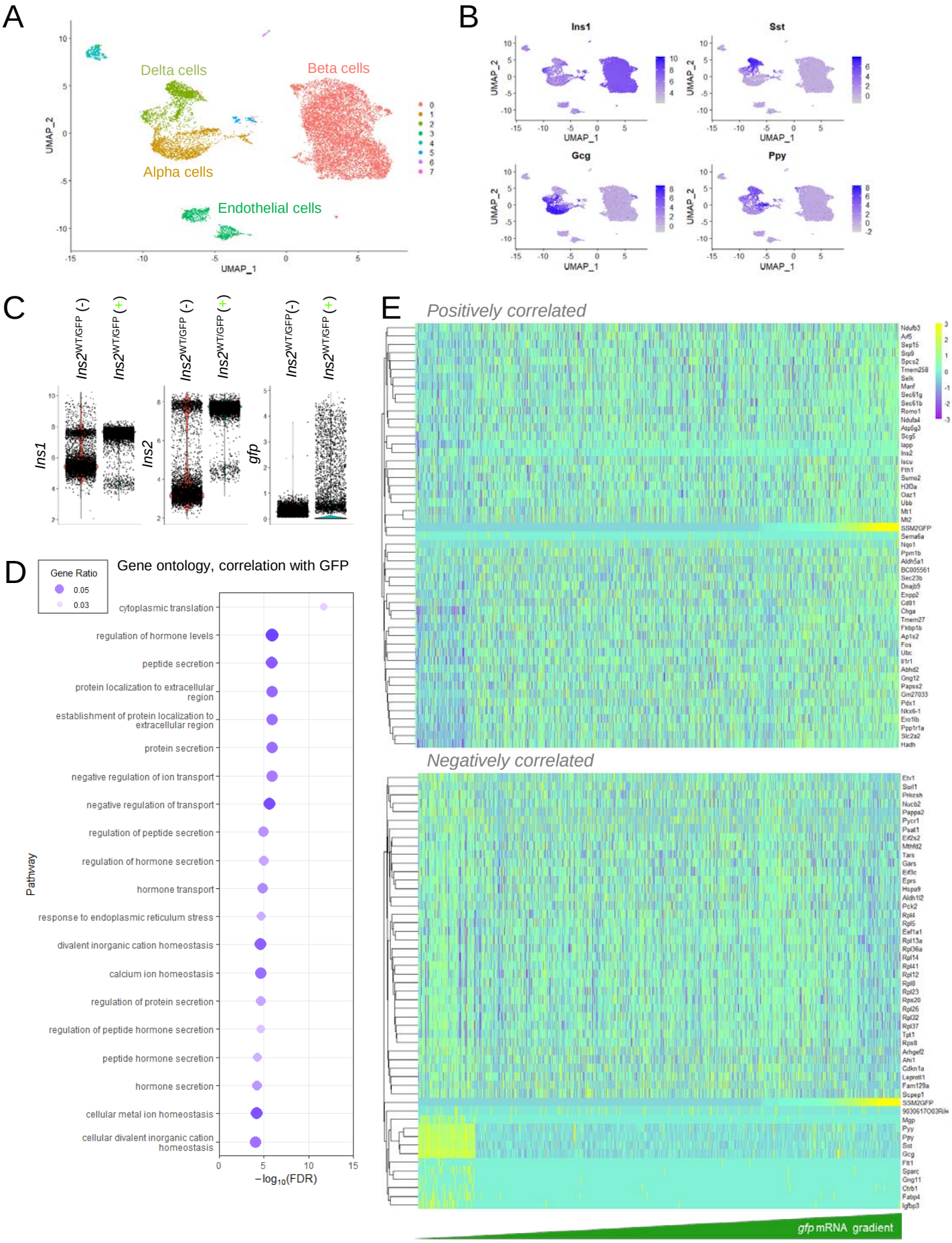
A
Delta cells
Beta cells
Alpha cells
Endothelial cells
UMAP_1
UMAP_2
B
Ins1
Sst
Gcg
Ppy
C
Ins2WT/GFP (-)
Ins2WT/GFP (+)
Ins1
Ins2
gfp
D
Gene ontology, correlation with GFP
Gene Ratio
0.05
0.03
cytoplasmic translation
regulation of hormone levels
peptide secretion
protein localization to extracellular region
establishment of protein localization to extracellular region
protein secretion
negative regulation of ion transport
negative regulation of transport
regulation of peptide secretion
regulation of hormone secretion
hormone transport
response to endoplasmic reticulum stress
divalent inorganic cation homeostasis
calcium ion homeostasis
regulation of protein secretion
regulation of peptide hormone secretion
peptide hormone secretion
hormone secretion
cellular metal ion homeostasis
cellular divalent inorganic cation homeostasis
Pathway
−log10(FDR)
E
Positively correlated
Negatively correlated
gfp mRNA gradient

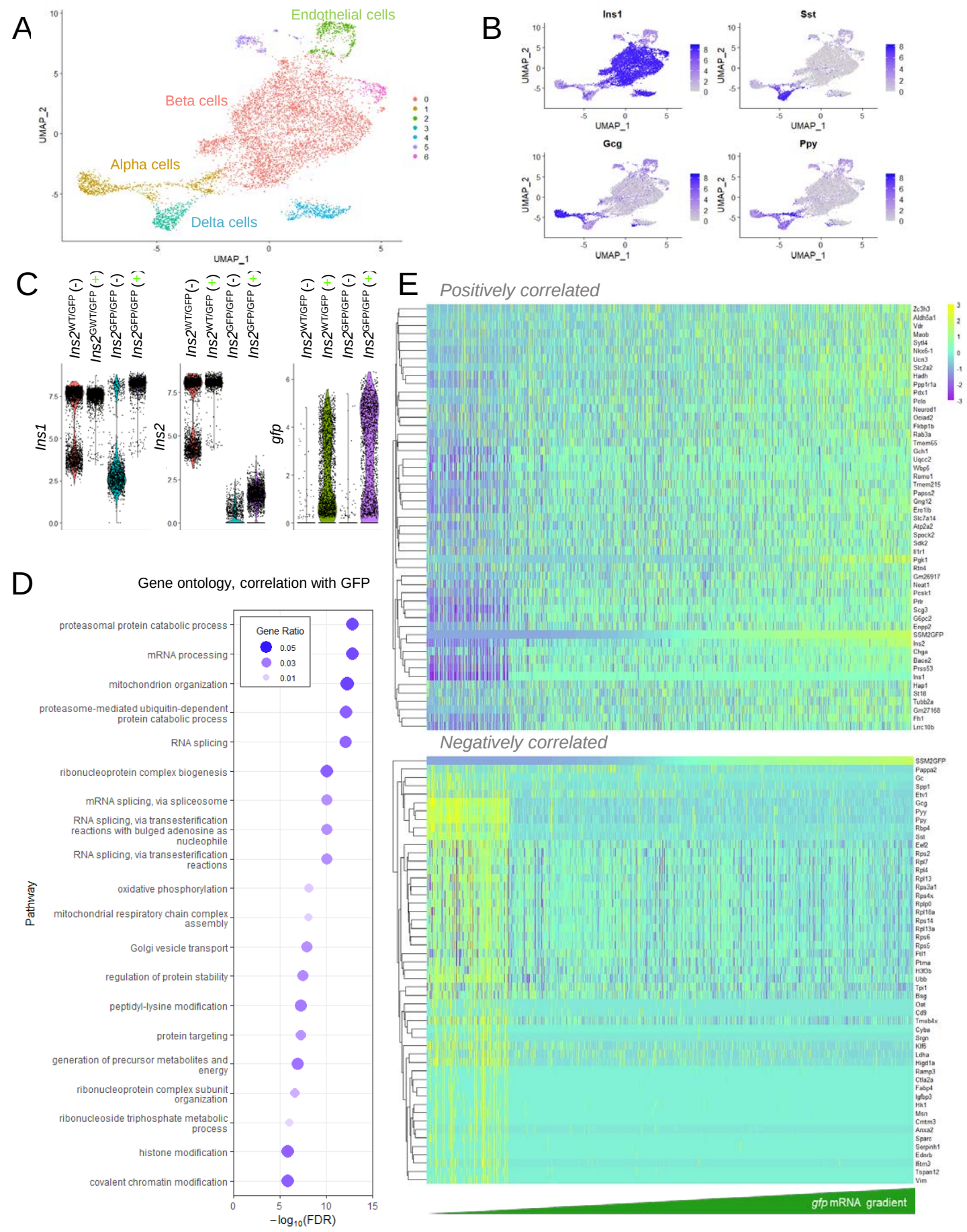
A
Endothelial cells
Beta cells
Alpha cells
Delta cells
UMAP_1
UMAP_2
0
1
2
3
4
5
6
B
Ins1
Sst
Gcg
Ppy
C
Ins2WT/GFP (-)
Ins2WT/GFP (+)
Ins2GFP/GFP (-)
Ins2GFP/GFP (+)
Ins1
Ins2
gfp
D
Gene ontology, correlation with GFP
Gene Ratio
0.05
0.03
0.01
proteasomal protein catabolic process
mRNA processing
mitochondrion organization
proteasome-mediated ubiquitin-dependent protein catabolic process
RNA splicing
ribonucleoprotein complex biogenesis
mRNA splicing, via spliceosome
RNA splicing, via transesterification reactions with bulged adenosine as nucleophile
RNA splicing, via transesterification reactions
oxidative phosphorylation
mitochondrial respiratory chain complex assembly
Golgi vesicle transport
regulation of protein stability
peptidyl-lysine modification
protein targeting
generation of precursor metabolites and energy
ribonucleoprotein complex subunit organization
ribonucleoside triphosphate metabolic process
histone modification
covalent chromatin modification
Pathway
−log10(FDR)
E
Positively correlated
Negatively correlated
gfp mRNA gradient

A

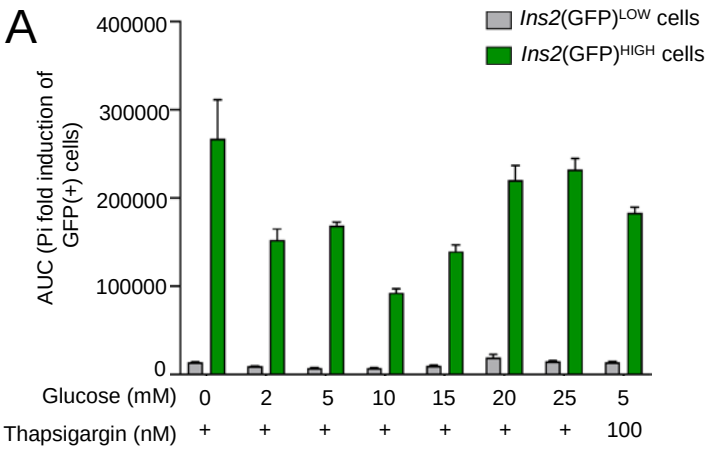
Ins2(GFP)LOW cells
Ins2(GFP)HIGH cells
AUC (Pi fold induction of GFP(+) cells)
400000
300000
200000
100000
0
Glucose (mM) 0 2 5 10 15 20 25 5
Thapsigargin (nM) + + + + + + + 100

B

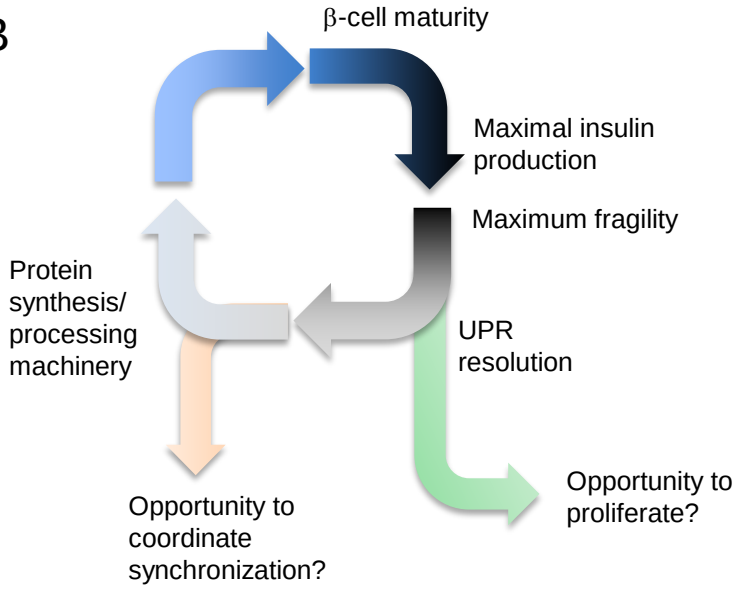
β-cell maturity
Maximal insulin production
Maximum fragility
UPR resolution
Opportunity to proliferate?
Opportunity to coordinate synchronization?
Protein synthesis/ processing machinery